RUPRECHT-KARLS-UNIVERSITÄT HEIDELBERG

Thomas Junkermann

# Timing Calibration and Validation of the Analogue Electronics for the Upgraded ATLAS Level-1 Calorimeter Trigger

Masterarbeit

HD-KIP-21-85

KIRCHHOFF-INSTITUT FÜR PHYSIK

**Department of Physics and Astronomy**
**University of Heidelberg**

Master thesis in Physics
submitted by

**Thomas Junkermann**
born in Worms, Germany

handed in on
**01.04.2021**

# Timing Calibration and Validation of the Analogue Electronics for the Upgraded ATLAS Level-1 Calorimeter Trigger

This Master thesis has been carried out by **Thomas Junkermann**
at the Kirchhoff-Institute for Physics in Heidelberg
under the supervision of
**Prof. Dr. Hans-Christian Schultz-Coulon**

**Timing Calibration and Validation of the Analogue Electronics for the Upgraded ATLAS Level-1 Calorimeter Trigger**

by Thomas Junkermann

## Abstract

During the Phase-I Upgrade of the ATLAS experiment, new electronic components get installed in the Liquid Argon front-end electronics to supply the Level-1 Calorimeter Trigger with a finer spatial granularity of energy depositions in Run 3. The Run 2 Level-1 Calorimeter Trigger system is further operated in Run 3. This is achieved with the newly installed Liquid Argon Trigger Digitizer Boards (LTDBs) which digitize the high resolution signals for the Run 3 system and also build the analog sums for the Run 2 system. The effect of the LTDBs onto the Run 2 Level-1 Calorimeter Trigger system is studied since they introduce a time delay for two of the four signal parts which are added up to the basic Run 2 Level-1 Calorimeter Trigger input, namely one Trigger Tower. This effect is measured and re-adjusted in the Tower Builder Boards to ensure correct input signals for the Level-1 Calorimeter Trigger. Additionally, the effects of the new electronics on the signal height and shape are studied.

**Timing Calibration and Validation of the Analogue Electronics for the Upgraded ATLAS Level-1 Calorimeter Trigger**

geschrieben von Thomas Junkermann

## Zusammenfassung

Im Rahmen des Phase-I Upgrades des ATLAS Experiments werden neue elektronische Komponenten zur Liquid Argon Elektronik hinzugefügt, welche eine bessere räumliche Auflösung der Energiedeposition bei der Auswahl von Ereignissen in Run 3 ermöglichen. In Run 3 wird das Run 2 Level-1 Kalorimeter Trigger System weiterhin betrieben. Die Liquid Argon Trigger Digitizer Boards (LTDBs) ermöglichen dies, indem sie die hochauflösenden Signale für das Run 3 System digitalisieren und die analogen Summen für das Run 2 Level-1 Kalorimeter Trigger System bilden. Die Installation der LTDBs zieht eine Signalverzögerung von zwei der vier Signale nach sich, die aufaddiert die kleinste Eingangsinformation des Run 2 Level-1 Kalorimeter Trigger bilden. Bei dem Addieren der vier Signale zu einem Trigger Tower Signal in den Tower Builder Boards kann diese Verzögerung ausgeglichen werden. Die verlängerte Laufzeit der Signale wird in dieser Arbeit bestimmt um damit die Tower Builder Boards zu konfigurieren. Darüber hinaus wird der Einfluss der neuen Elektronik auf die Höhe und die Form der Trigger Tower Signale untersucht um eine problemlose Funktion des Trigger Systems bezüglich der oben genannten Aspekte in Run 3 zu gewährleisten.

# Contents

# Motivation

The search for the most fundamental building blocks of ourselves and our surroundings is a task which has governed mankind for a long time and still is. Having started at the latest when in 1869 Dmitri Mendeleev first proposed the periodic table to bring order into the landscape of chemical elements, the hunt to identify and classify atoms, back then to be thought the basis of nature, began.
Soon after it turned out that atoms are not the fundamental building blocks of nature and first smaller particles like the electron were found. From that point on the race to find these fundamental particles started and eventually ended up in today's modern understanding of the Standard Model of Particle Physics. In this process, there have been various attempts to find new particles and different concepts of so called particle accelerators have evolved. With finding more and more particles of the Standard Model of Particle Physics and wide energy ranges being covered by accelerators, the technical challenges of building these to perfection kept rising. Having peaked in today's Large Hadron Collider, a circular particle collider in Geneva, key features of the Standard Model of Particle Physics like the Higgs boson were verified recently. Always aiming for a better understanding of physics, the LHC and its experiments, like ATLAS, receive regular updates to exploite modern technology to its best. ATLAS and its Level-1 Calorimeter Trigger are currently receiving an upgrade, which will improve spatial resolution of energy deposition when selecting events during data taking. This update changes electronic components and therefore requires checks if signal pathing and construction is maintained as desired. Verifying this and performing further tests on the updated system are the motivation for the following work.

# Chapter 1

# Introduction

This chapter serves as an introduction to the structure and the topics covered in this thesis. A short introduction to the LHC and its most important properties is given. Afterwards, the structure of the ATLAS detector, which is the experiment the studies of this thesis are based on, is explained.

Having set the overall scene for this thesis, chapter 2 will pick up the line of thought and dive into the ATLAS detector. In chapter 2 the ATLAS electronics, subsystems and components used in this thesis will be described. An understanding for the so called front-end electronics, electronics directly mounted on the detector, will be build and important parts of the Level-1 trigger hardware will be mentioned. Additionally, the connection and functionality between these systems is shown. Chapter 2 also lays out the concept of the so-called Phos4Scans which are used for timing calibration while the detector is not running and shows how these signals are created.

One of the most important tasks of this thesis is to derive new Tower Builder Board delays due to the introduction of new electronic components. This is described in chapter 3. The Phos4LayerScans are used to derive the aforementioned delays and the general accuracy of the time measurement is given.

Chapter 4 focuses on whether the change in electronics and signal path has an influence on the shape of the calibration signals. Parameters like signal height and width (or rise time) are presented and compared to previous

versions of the experimental setup. Changes visible here are then investigated upon their impact onto the trigger system.

The last chapter of this thesis, chapter 5, presents the effects of lost signal height in different runs and necessary adjustments to the gains counteracting these are proposed. For this, another concept of special runs, namely short and long energy ramps, is presented and shown.
In the end all studies will be summarized and interpreted in a conclusion and an outlook on necessary work which has to be done in the future will be given.

Multiple attachments build the end of this thesis. The first one, Appendix A, are first preliminary results regarding Tower Builder Board Delays in the EMBC. The second attachment, Appendix B, will feature a list of all abbreviations used in this work.

## 1.1 The ATLAS Experiment at the Large Hadron Collider

The ATLAS experiment is one of the four large experiments at the LHC (Large Hadron Collider) at CERN (Conseil européen pour la recherche nucléaire). The facilities of CERN are located next to Geneva and spread across the border between France and Switzerland. The LHC is a circular particle collider where mostly protons, at times also heavy ions, are accelerated in bunches, each holding $1.15 \cdot 10^{11}$ protons [1], making up a high-energetic particle beam. The LHC is the largest particle collider and its beams are the most energetic in the world with around 6.5 TeV per beam. Furthermore, it is operating with a collision frequency of up to 40 MHz, leading to the individual bunches in a beam to only be separated by 25 nanoseconds from another. There are always two beams being accelerated in opposite direction. These counter revolving beams can be forced to collide within the large experiments and the resulting particle collisions are observed.
To handle the vast amount of particles produced and therefore data to be recorded, there is a need for sophisticated algorithms and hardware with which the data can be filtered in real time such that only interesting events,

potentially including new insights into physics, are permanently stored. This is done by the trigger system which will be covered in section 2.2.7.

## 1.2 The ATLAS Detector

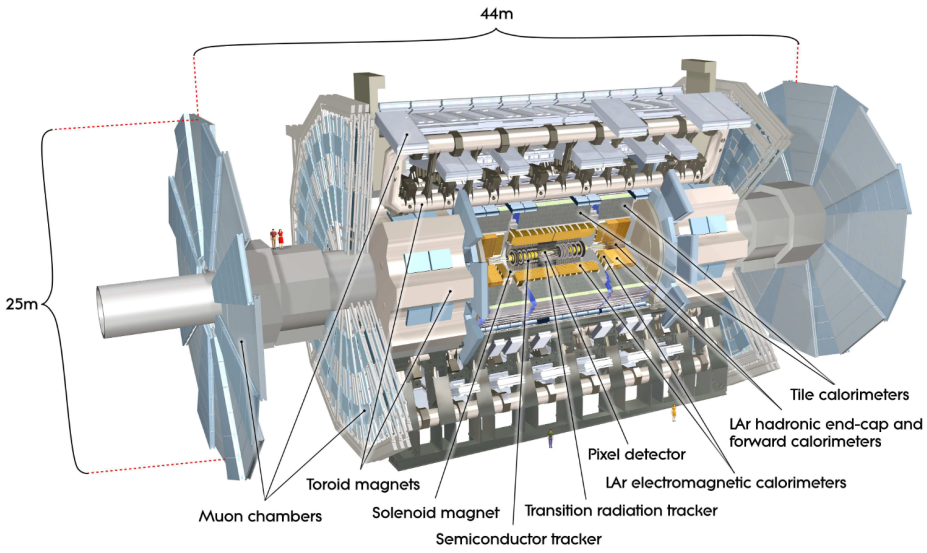


Figure 1.1: The ATLAS detector with its subsystems, taken from [2].

The ATLAS detector has a cylindrical shape and is generally build up in layers. In the very center, right around the point where the protons collide, is the inner detector. It measures direction, charge and momentum of charged particles. The tracking systems inside the inner detector allow to precisely measure particle tracks. Large solenoid magnets produce a magnetic field of 2T for the inner detector. Outside the inner detector, two calorimeters are located. The first one being the electromagnetic calorimeter (ECAL). It is a sampling calorimeter using Liquid Argon as active medium and lead as a absorber to shower incident particles. The ECAL, which surrounds the inner detector, measures the energy lost by photons and electrically charged particles, mostly electrons and positrons, traversing through it. The electromagnetic calorimeter is composed of three or four layers (presampler, front, middle and back layer, from inside to outside) which will become important later on. The presampler is only present for $\eta < 1.8$, [3]. Around the electromagnetic calorimeter lies the hadronic calorimeter (HCAL) measur-

ing the energy of all hadrons. These calorimeters are so dense that they are able to stop nearly all particles, except for muons and neutrinos. Forward calorimeters are installed close to the beam axis far from the point of collision. They allow for energy measurements of particles being emitted close to the beam axis and therefore not being caught by the other calorimeters. The outermost part of the ATLAS detector is formed by toroid magnets and muon detectors. The magnets bend the trajectory of muons which are subsequently detected by the muon spectrometer.
To navigate inside the detector and communicate results between the subdetectors there are different ways how the detector is mapped. The general form is the following.
The z-axis lies along the particle beam. The x-axis is pointing towards the center of the LHC and the y-axis points upwards out from the collision point. The coordinate $\phi$ describes the azimuthal angle around the z-axis. The coordinate $\eta$, called pseudo-rapidity, is defined as

$$\eta = -ln\left(tan\left(\frac{\theta_{cm}}{2}\right)\right) \ , \tag{1.1}$$

with $\theta_{cm}$ being the polar angle in the center of mass system of the colliding protons. $|\eta|$ ranges from 0, pointing along the y-axis, towards infinity for which it points into the x-z-plane (negative $\eta$ values describe the opposing side of the detector). Using these coordinates has the important advantage that they build a coordinate system that can be easily represented in two dimensions with $\eta$ on the x-axis and $\phi$ on the y-axis when displaying results. A point in this coordinate system can thus represent a direction in which a particle is leaving from the center. This mapping is used throughout this thesis. There are further methods to locate specific points in the detector. It is common to also specify areas in the detector by referring to the electronics built within the respective area. One frequently used example will later be explained in section 2.2.7.

## 1.3 Runs and Shutdowns

The Large Hadron Collider is not running full time each day of the year. Verification and monitoring of the machinery is crucial for experiments of this size. Therefore, at times the experiment needs to be shut down, ei-

ther partially or fully, to perform checks on all the different components. For example, each winter there is the Year-End Technical Stop, the YETS, where maintenance can take place in the accelerators and beam lines. The experiments are also maintained and repaired during this time, there are no upgrades in this time though.

The first time ever when protons were accelerated through the full length of the LHC was in September 2008 where test runs where done with very low injections and energy. An incident in late 2008 delayed first real runs to late 2009 where in November the previous record for the beam energy was broken with 1.18 TeV thus making the LHC the highest energy particle accelerator. During Run 1, started in late 2009, energies were continuously increased and in March 2010 a center of mass energy of 7 TeV was reached for the first time. Due to its outstanding performance, Run 1 was prolonged by 1 year from late 2011 to early 2013. This was also motivated by the possible discovery of the Higgs Boson to collect more data, [4].

From early 2013 to April 2015 followed the first long shutdown, LS1. During this shutdown the general accelerator structure was upgraded to be able to originally reach center of mass energies of up to 14 TeV in Run 2 starting in 2015. Though, most of the time in Run 2 13 TeV have been used. The experiments and the L1Calo Trigger also received upgrades. Luminosity has also been increased greatly during Run 2. It even has reached beyond expectations with 10% above the targeted luminosity for ATLAS and CMS, see [5].

In December 2018 Run 2 ended and long shutdown 2, LS2, began. The goal of LS2, which is currently taking place, is to implement first hardware for the High Luminosity Large Hadron Collider, further increasing the luminosity in the future, as well as upgrades inside the experiments. One of the upgrades in ATLAS is the introduction of the so-called Liquid Argon super cells (for a detailed view, see [6]), allowing for higher spatial resolution for energy deposition in the trigger systems responsible for the electromagnetic calorimeter. The verification of the functionality and performance of these new hardware components are a major part of this work.

# Chapter 2

# Hardware Background and Analysis Methods

This second chapter of this thesis aims to build an understanding of all electronic components relevant for the studies presented in chapter 3 to 5. These are mostly from the front-end electronics of the electromagnetic calorimeter as well as the Level-1 Calorimeter (L1Calo) Trigger of the ATLAS experiment. Explaining these in detail helps to understand their functionality between one another. The first sections present the setup used in Run 2, before in section 2.4 the Run 3 setup is shown and its differences highlighted. Beyond that, further technical concepts, including special test runs, are introduced and their features explained.

## 2.1 Signal Path in Run 2

Figure 2.1 shows which path the signal takes after the energy deposition is measured in the calorimeter cells, the 'Electrode' seen at the very bottom, through the front-end electronics into the Level-1 Calorimeter Trigger (on the top right). It can be seen that the raw signals coming from the single calorimeter cells are first running through a preamplification. After this an important split in the shaper chip is happening.
On one path, the read-out path, the signals are further amplified and after that sampled, with the LHC bunch crossing frequency of 40MHz, and stored for a short period of time (equivalent to the Level-1 latency) in the switch-capacitor arrays, the SCA. Buffering the signals for a short time allows for

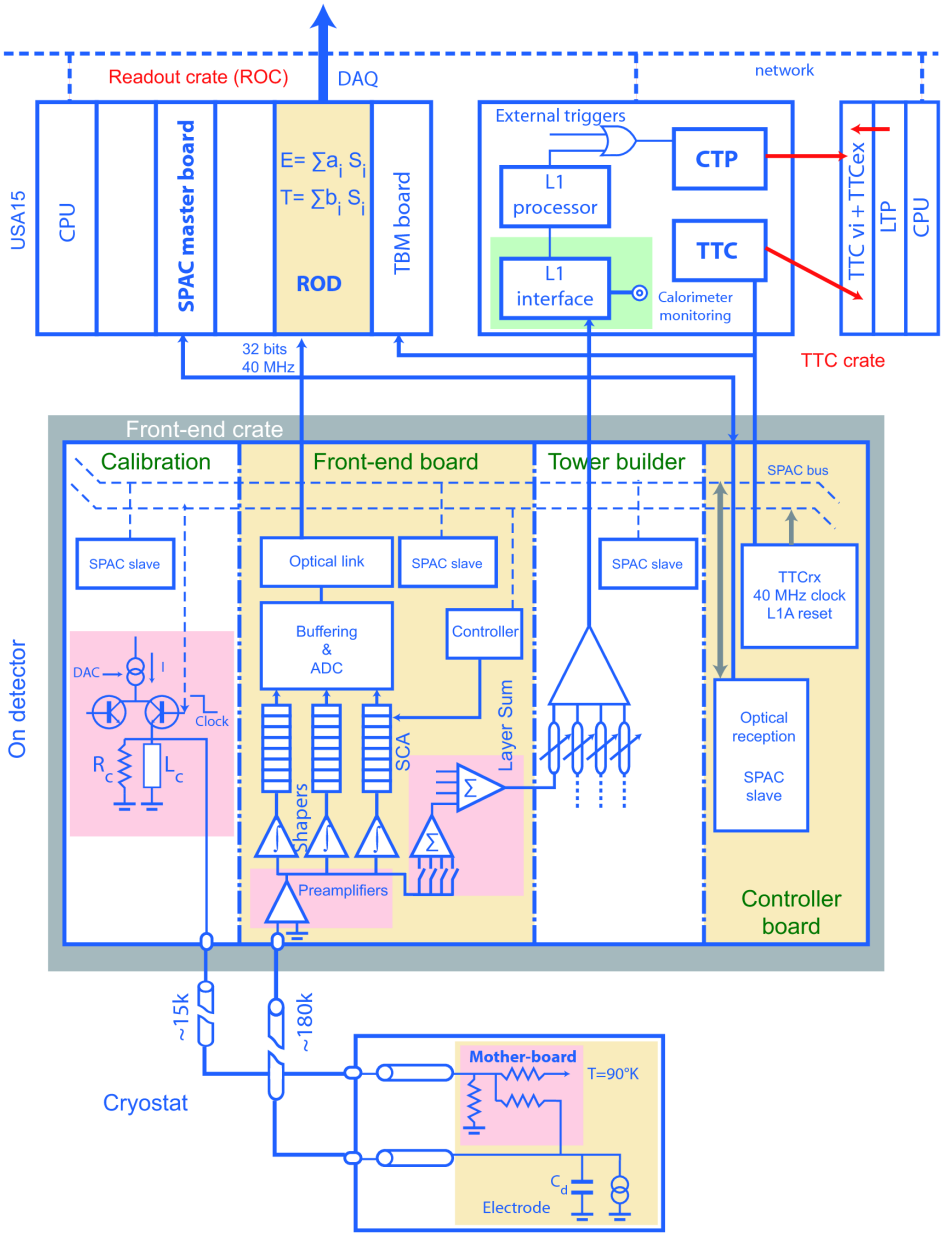


Figure 2.1: The Liquid Argon front-end electronics from Run 2 are shown together with the back-end system, taken from [7].

the second path, the trigger path, to transfer the signals to the Level-1 Calorimeter Trigger and the Central Trigger Processor which process them. After the signal leaves the SCA, if the corresponding event is accepted by the level one trigger, it is further processed on the read-out path, by e.g.

converting it to digital form and formatting it. This will then send it to the read-out systems (RODs). It is important to note here, the above picture suggests that the signals for the L1 Calorimeter Trigger are split off before entering the shaper, this is not true, the split takes place inside the shaper chip.
The front-end electronics are also responsible for building so-called trigger towers. All analog elementary cell signals within $0.1 \times 0.1$ in the eta-phi space (for $\eta < 2.5$, outer regions have larger towers) are summed up to form one trigger tower, which is the most basic input for the L1 Calorimeter Trigger. This happens on the already mentioned trigger path which is the one leading to the L1Calo Trigger system. Here, the signal is routed from the shaper chip towards the layer sum boards, adding up the signals from multiple shaper chips to one layer of a trigger tower. After that, the output of the layer sum board is driven through the base plane of the front-end crate to the Tower Builder Board. There, the energy sums of the four different layers are added up to from one trigger tower signal that is proportional to the transversal energy $E_T$, deposited in the region of that trigger tower. After passing this last step in the front-end electronics the signal is routed to a distant cavern, called USA15, where the Level-1 Calorimeter trigger, together with all other electronics not mounted directly on the detector, is located.
After this brief overview of LAr components and L1Calo Trigger and where they are located in the signal path from the calorimeter cells through the front-end electronics into the back-end, they are now presented and their use during testing explained in greater detail.

## 2.2 Electronic Elements

### 2.2.1 Calibration Board

During the long shutdown no beams are accelerated and therefore no usual physics signals are being produced which can be used to test new detector parts. To verify newly installed electronic parts before actual physics data taking starts in Run 3, there are ways to inject specific pulses into the calorimeter electronics to reproduce the real physics signals as closely as possible. This also has the large advantage of maintaining high control over what is injected and therefore expectations can be made of what the

systems should read out. This then allows to calibrate the system to very high precision.
The calibration board can be found in the LAr front-end crate (see figure 2.1). With the help of a DAC (Digital to Analog Converter) we are able to tell the board how large injected signal should be. The calibration board is connected to the timing control of the front- and back-end system and uses the 40MHz clock of the LHC. The calibration signals, created in the calibration board, are then send as close as possible to the origin of the real physics signals, i.e. the electrodes inside the calorimeter. This ensures that the calibration signal undergoes the exact same steps as the physics signal and that there is no difference in electronic modification. The fact that they are created differently, therefore having slightly different shape, can be taken into account at a later step in the signal path.
The calibration board is therefore of great importance because all the signals used in this work and for general calibration of the LAr and L1Calo Trigger system are initially generated by this board.
Specifying what the test should achieve it is possible to run various routines during calibration. The individual elementary cell signals will always be of the same form but can be adjusted in the energy deposited via the DAC. Furthermore individual cells as well as arbitrarily many can be pulsed at once. The for this work important Phos4Scans and their signal generation is later described in section 2.3.

### 2.2.2 Preamplifier

Preamplifiers, placed on the front-end board (FEB), amplify the raw signal above noise level of electronic elements further down the signal path. The preamplifiers are also cleverly matched to the following shaper chip, presented in section 2.2.3, and the read-out electronics. They amplify the signal in a way to fit the output signal into the dynamic range of the shaper and read-out.

### 2.2.3 Shaper Chip

As seen in figure 2.1, the shaper chip is the first more complex component the signals from the ECAL enter on the front-end board, after running through a preamplification. The shaper chip has multiple tasks assigned to it. The

first one being the splitting of the signal for the aforementioned different paths it takes from here, once to the read-out and the other to the L1Calo Trigger. One other major task the shaper handles is dealing with the 16-bit input signal coming from the calorimeter cells. The pipeline following the shaper chip, which stores the signal during the L1 latency, and the digitization system are both based on 12-bit precision. Therefore, the shaper provides three different gain scales, each having a 12-bit range, to not loose information and precision from the 16-bit initial signal. The gain scales are related to one another by a factor of 10.
The shaper, hence its name, also shapes the signal by differentiating and integrating it. For this, it uses a bipolar CR-$(RC)^2$ circuit. The effect and result of the modification to the raw signal can be seen in figure 2.2.

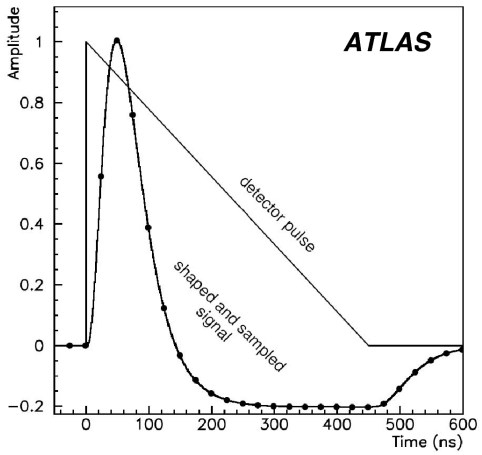


Figure 2.2: The original calorimeter signal is shown together with its shaped form. The dots represent the shaped, sampled and digitised signal which gets read out from the SCA, taken from [7].

In addition the shaper also limits the system bandwidth to match the 40 MHz sampling frequency of the switch-capacitor arrays. Furthermore, the shaper also performs a first analog sum of its four input channels for the signals following the path towards the trigger.

### 2.2.4 Switch-Capacitor Array

The signals leaving the shaper are sampled and stored in the switch-capacitor array at 40 MHz. The sampling clock is aligned in a way ensuring that one sample is always taken at the maximum amplitude of the signal. The switch-capacitor array is chosen large enough for it to store all events during the latency of the level-one trigger, which is 2.5 $\mu$s at maximum. If an event is found to be interesting by receiving a Level-One Accept signal it is digitized and sent to the read-out system in the back-end electronics. The Level-1 accept signal is sent from the central trigger processor, the CTP, and is driven back to the front-end via the timing trigger and control system, the TTC.

### 2.2.5 Layer Sum Boards

For this work, the path of interest is the second one out of the shaper chip, the path of the signal through the analog summation to one trigger tower. The first step of summation is done by the shapers adding their four input channels. Here, it is important to note that cells from the different layers of the electromagnetic calorimeter, covering the full depth of this detector component, are never mixed in one front-end board. One front-end board always contains only signals from cells in one layer. This makes it easier to sum these cells into one layer by the Layer Sum Board, plugged onto the front-end boards, since no modification or adaptation for signal shape or gain is needed. This is not generally the case. Signals from different layers can vary so far from one another where factors like shape, gain or timing need to be accounted for. This is handled by the Tower Builder Boards, which sum up layer signals, coming from different layer sum boards, to one trigger tower.

### 2.2.6 Tower Builder Boards

After the signals of the different cells have been summed up into the four layers they are routed through the front-end crate base plane to the Tower Builder Boards (TBB). These have multiple functions. The main task of these is adding up the signals of the four layers to make up one trigger tower (TT) signal. This summation of the analog signals is ideally performed when the points of maximum height of the layer signals are overlapping in time since the signal height is proportional to the transverse energy in that layer.

One trigger tower signal should consist of the correct energy of all four layers of that given tower and therefore it would be fatal if the signal peaks of the different layers are not aligned in time.
This is taken care of by another key feature of the Tower Builder Boards. A certain delay for each individual layer can be introduced by loading it from the Tower Builder Board database. There are databases for each region of the detector always containing entries for each layer of every trigger tower. If all the layers should run parallel in time, i.e. the maximums of the analog signals for all four layers coincide in time, there is no need to introduce a delay. For stability reasons it is preferred though, to then shift all the layer signals to the same high delays.
Another important point to mention concerning the Tower Builder Board's database is that there are always two complete and independent sets of databases. This is due to one of them being a database for actual physics runs and the other one being used in calibration and testing. These are already filled with the delays from Run 2 and are not emptied for Run 3. Having two sets of databases is very important. The consequences of this are explained in the following section 2.4 concerning testing and deriving the TBB delays.
The Tower Builder Boards are built in a way where they can shift the layer signals by multiples, so called ticks, of 2.5 nanoseconds. It is possible to shift from 0 nanoseconds up to $7 \cdot 2.5$ ns = 17.5 ns. Smaller steps are not possible and if studies show a necessary shift of for example 6.5 ns the delay gets rounded to the next closest multiple of 2.5 ns which would be 3 ticks corresponding to 7.5 ns.
There are further features like the possibility to introduce a certain gain to layers or distort their shape in the Tower Builder Boards. They are, however, not the key to understand the work which is carried out here and therefore omitted. For a more detailed look [3] is recommended.
Having created full tower signals in the front-end, these get transferred to the Level-1 Calorimeter Trigger in USA15.

### 2.2.7 Level-1 Calorimeter Trigger

The ATLAS Level-1 Calorimeter Trigger is part of the two level trigger system from Run 2. It identifies physics objects, like electrons, photons, and jets using hardware based algorithms using information coming from the

calorimeters. In this first level of identification, only reduced information is used since not every individual elementary cell enters the algorithms but rather multiple cells summed to a trigger tower as seen previously. This coarser spatial energy resolution is needed to be able to process information per event as fast as required, keeping the latency low in Run 2. The Level-1 Calorimeter Trigger reduces the event rate to 75kHz. The identified object information is transmitted to the Central Trigger Processor which then decides whether a Level-1 trigger accept signal is sent. The second level is called the High Level Trigger which is based on software and further reduces the event rate to 1 kHz. It reconstructs the events using full granularity in regions of interest (RoI) derived by the L1Calo Trigger.

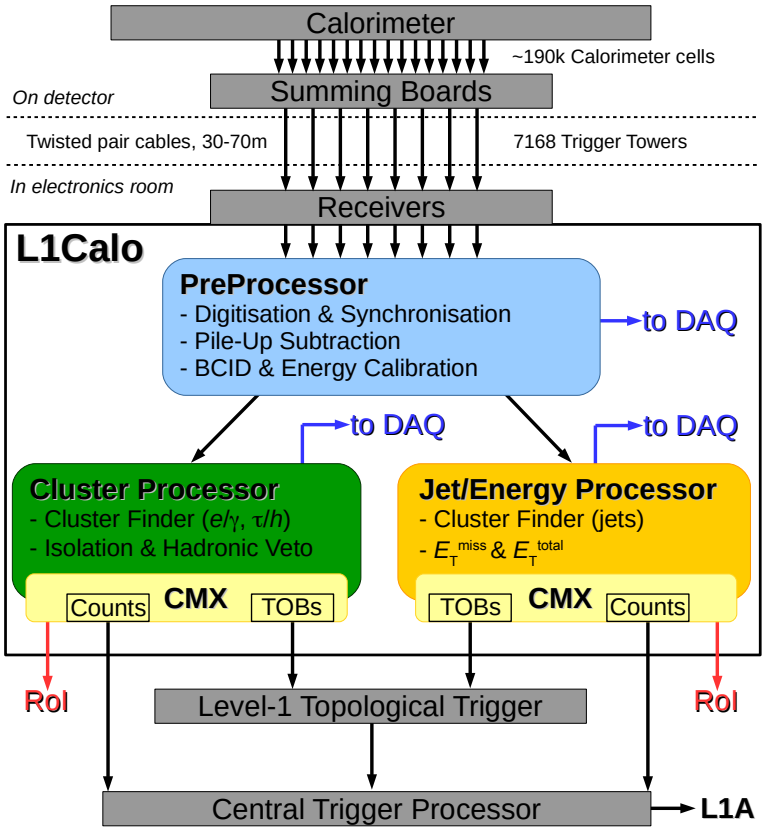


Figure 2.3: The Level-1 Calorimeter Trigger is shown together with its subsystmes taken from [8].

Inside the Level-1 Calorimeter system the first component the signals enter is called the PreProcessor. It prepares the digital data for the sub-

sequent components in the chain of the trigger system. One of the major components on the PreProcessor Module (PPM) is the Multichip Module (MCM or nMCM since Run 2) which assigns a transverse energy to the trigger tower signals and assigns all trigger tower signals to their corresponding bunch crossings. The trigger tower signals need to be synchronized up to one nanosecond for bunch crossing identification and transverse energy assignment. Further components in the L1Calo Trigger are the Cluster Processor which looks for electrons, photons or tau candidates as well as the Jet/Energy Processor which identifies jets and calculates total and missing transverse energy, [9]. The synchronization of TT signals is done via the PreProcessor Module Input Timing. This input timing can be set by multiples of one nanosecond and allows the subsequent system to precisely know when the signals arrive.
This input timing needs to be adjusted after timing changes have been applied to the signal earlier, like introducing new Tower Builder Board delays. The way this is done is explained in section 2.6. The trigger towers that are used within the L1Calo Trigger carry a unique identifier: the COOLID. Each trigger tower has a individual COOLID made of the specific number for the PreProcessor crate where the electronics responsible for it are located, the PreProcessor Module number inside that crate, the MultiChip Module number inside that module and the MCM channel. The COOLID is build in the following way

$$COOLID = 0x0 + \text{Crate} + 1 + \text{PPM} + 0 + \text{MCM} + 0 + \text{MCM Ch.}\ , \quad (2.1)$$

where Crate, PPM, MCM and MCM Ch[annel] are the corresponding internal numbers in hexadecimal form. The overall crate is literally the crate holding most of the L1Calo Trigger components in place. There are eight crates with numbers 0 to 7. The PreProcessor Module has been mentioned previously and numbers range from 0 to f (15). The MCM is one component on top of the PPM processing signals. There are 16 MCMs on one PPM, numbers therefore ranging from 0 to f and each MCM has four channel processing four TT. These are the MCM channel numbers from 0 to 3.
An example for a COOLID for a trigger tower is 0x01180101. This is the trigger tower in the PreProcessor crate 1, processed by PPM eight and MCM one routed through MCM channel one.

## 2.3 Phos4Scans

Phos4Scans are essential to the work in this thesis and are one of the main tools used to create the signals. During Phos4Scans pulses are injected into the system through the calibration board as if they were created by the calorimeter cells themselves. Individual cells can be pulsed as well as an arbitrary amount of cells at once. The 'events' are read out by sending a manual L1Accept signal. The special feature about Phos4Scans is that they produce an processed output signal with one nanosecond resolution in contrast to the normal read-out being only digitized every 25 nanoseconds. This resolution is achieved by first injecting 200 pulses into all cells, reading them out and after that stopping the injections for a short amount of time to shift the digitization clock of the ADCs by one nanosecond. After that the injections continue and after 200 injections they are stopped again and the digitization clock is shifted by one more nanosecond. This is repeated 23 more times. After having recorded these signals, all of the 200 equally timed signals are averaged and the 25 averages are overlapped into one signal. Overlapping the signals which are digitized in different points in time therefore allows for this high resolution while making use of standard read-out.
Another variation of this are the Phos4LayerScans. When creating these, only cells from one layer in depth of all the trigger towers are pulsed. This allows to read out the layer sum signals instead of trigger tower signals, making it possible to compare the layer signal between one another.
One of the largest benefits of Phos4LayerScans is the individual read-out of different layers. In usual physics data taking this is not possible since all layers are summed up together. To deal with this in physics, special runs, for example end-of-fill studies, would need to be dedicated to derive the time delays where essentially three of four layers are shut off in the analog sums. This, however, makes the trigger worse and data will not be properly recorded and therefore be useless for analysis of collisions. Furthermore, the physics signal would need to be fitted with established functions since they are only digitized every 25 nanoseconds.

## 2.4 Run 3 Electronics Changes

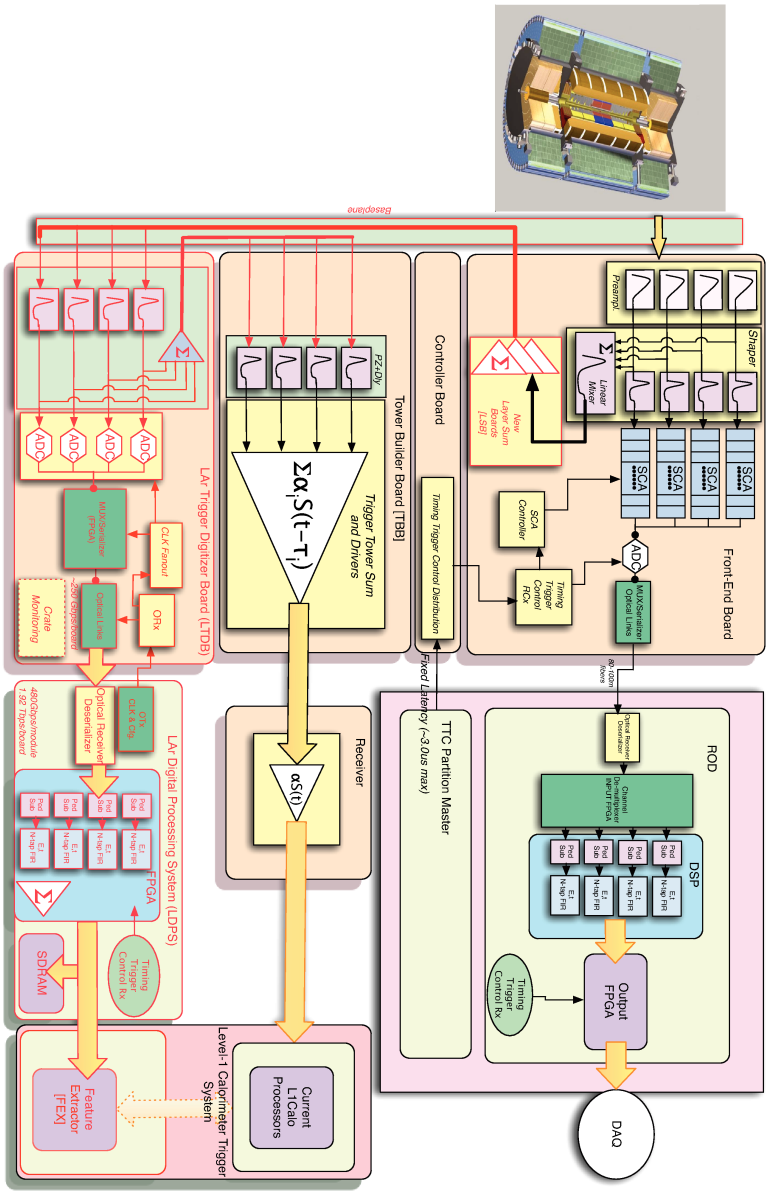


Figure 2.4: The upgraded LAr front-end electronics are shown together with the back-end systems. Components which are upgraded or newly introduced are marked with a red border, taken from [7].

Above picture, figure 2.4, shows the newly introduced LAr trigger electronics during the long shutdown 2, e.g. the LTDB (Liquid Argon Trigger Digitizer Board) and LDPS (Liquid Argon Processing System). All new

components in Run 3 are marked by a red border. These are necessary to provide the Level-1 Calorimeter Trigger system in Run 3 with higher spatial enery resolution. In Run 3, information will not be restrained to trigger tower granularity but a resolution that is increased by a factor of ten. The Run 2 system will be kept and run in parallel to compare the new system against the old one, which is well-understood and established, and to have a backup solution if the newly introduced electronic components do not allow a smooth data taking.

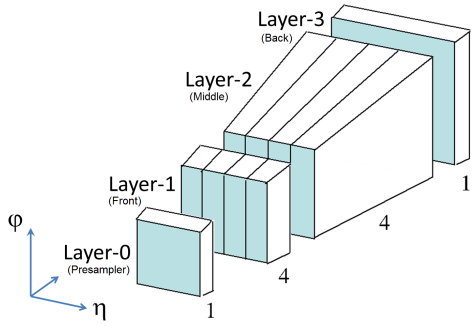


Figure 2.5: The new super cells with ten times finer spatial resolution than one TT are shown. In Run 2, four layer sums have been built to one TT. In Run 3, the new layer sum boards build 10 smaller sums for the digital trigger path. Taken from [6].

The higher spatial resolution in energy deposition brings further changes with it. In Run 3 one trigger tower is built, but two of the four layers have four times better resolution. This is achieved by not summing up cells corresponding to the front and middle layer into these layers but eight smaller layer, the super cells. The presampler and back layer are unchanged and will still be summed up as in Run 2 but also used in the digital trigger as super cells. Therefore, there are also new layer sum boards introduced which perform the summation of all elementary cells to the desired spatial resolution. These new super cells are propagated by the new path through the LTDB and LAr Digital Processing System (LDPS). In the old Run 2 system, which will run in parallel in the beginning of Run 3, the inputs for the TBBs need to be delivered in their nominal spatial resolution, i.e. for the central region layers with 0.1x0.1 in eta-phi. For this there are further sums performed on the LTDB, summing the new super cells back to the old

front and middle layer, indicated by the sum symbol in figure 2.4 inside the green of the LTDB. Regarding the presampler and back-layer, they directly enter the Tower Builder Board after the LSBs, like in Run 2.

## 2.5 Tower Builder Board Delay Changes

As seen in section 2.4, due to the presampler and back layer signals taking the direct route into the Tower Builder Board and the front and middle layer signals needing to travel a longer distance through the LTDB first, a delay between these two sets of layers is introduced. This needs to be accounted for in the Tower Builder Boards by adjusting individual layer delays with corrections.
These corrections to the delays necessary between the different layer are calculated in chapter 3. Optimizing the calculated corrections for the Tower Builder Board database is done by Liquid Argon using an algorithm which takes the delays as input. The optimization is done for all layers at once. The algorithm also cancels the necessary shifts out against each other, if possible, and tries to find the best way of implementing the shifts. As an example, if three layers would need a shift of one tick in front of the middle layer, it would be possible to shift the middle layer back by one tick instead. As previously mentioned it also takes into account that the delays are preferably set to high ticks. Therefore, the delays of all layers are pushed up by the largest amount of ticks possible. This amount is given by the layer which is closest to 7 ticks. It can occur that a correction is needed which cannot be accounted for since the tick range is limited between 0 and 7 ticks. However, this is rarely the case and often has no large effect. This can be illustrated by looking at one layer within a TT which needs a delay of 3.9 ns, which would be 2 ticks, but only 1 is possible due to limitations set by the other layers (this could be one layer already sitting at 0 ticks and no relative shifts of the other layer towards this layer are possible). The delay for this layer would be 1.4 ns off from the nominal value, which is acceptable. Why this is the case will be discussed in chapter 3.
In section 2.3, it was explained that special Phos4LayerScans can be used to read out the individual layers for each trigger tower. This allows for using the usual Level-1 Calorimeter Trigger read-out and still only obtain information about that layer since it is not mixed (i.e. summed by the

TBB) with the other three layers. More importantly, it is possible to compare the properties of the injected signals in each layer with one another since the same read-out can be used. This is possible since the procedure of creating these Phos4LayerScan signals is precise enough to acknowledge conditions for all layers, i.e. four calibration runs, are equal. Using these special Phos4LayerScans with one nanosecond resolution allows to read out the layer signals for each trigger tower and compare them against each other. The middle layer is chosen as the reference layer since most of the energy of an electromagnetic shower will be deposited here.

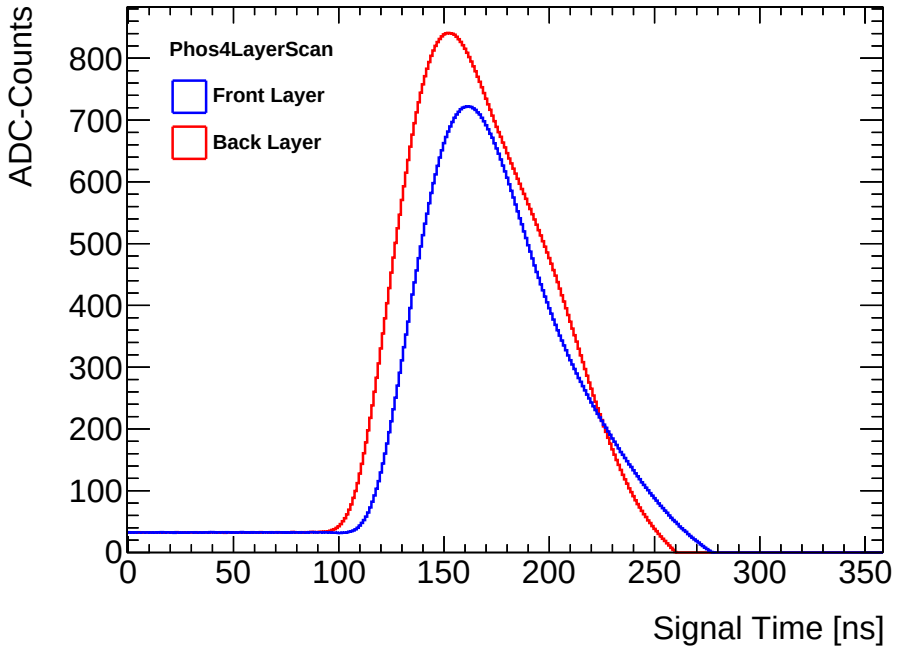


Figure 2.6: The final read-out from two Phos4LayerScans for the front- and middle layer of trigger tower 0x0100702 is shown.

The property of interest to compare the signals is their time of maximum amplitude. The difference in time between the layers times of maximum amplitude is extracted. An example is visualized in figure 2.6. Shown is the time difference between the injected signals in the front- and back layer for one specific TT due to the newly installed LTDBs. The difference in amplitude of the two layers is owed to the fact that they are different layers and thus have a different amount of elementary cells to them. The difference in

peak time is now rounded to multiples of 2.5 ns and subsequently divided by 2.5 ns to obtain the number of ticks necessary to align the layers. This is done for every layer and every trigger tower and the ticks are proposed as a correction for the already existing Tower Builder Board database.
Problems arise in usual data taking runs, or physics runs, where above procedure of deriving a delay is not possible anymore. First of all, the physics pulses are digitized every 25 ns. Therefore, their resolution in time is not as high as the resolution of test signals obtained with the Phos4LayerScans. To cope with this, an approximation of the peak position of the signal pulse can be found by fitting physics pulses with established fit parameters from Run 1 and then use the time of maximum amplitude. Further issues arise since in usual data taking the layer signals of one trigger tower are not read out. This can only be achieved by masking the layers via the shaper, i.e. 'turning off' certain layers for triggering. Doing so, results in a worse trigger since the energy the trigger sees is heavily reduced and less events are recorded. The problem with this is that there needs to be data for every trigger tower. At the very beginning of Run 3, the LHC will run with a low luminosity and only few collisions. Therefore, it will take time to derive reference data for the entire electromagnetic calorimeter. If, however not avoidable, for example due to bad legacy trigger performance, it is nonetheless possible to perform this procedure of deriving TBB delays in end of fill studies.
To avoid this and keep early data available, it is planned to predict the changes needed for the physics database based on changes applied to the calibration database which have been checked and verified through Phos4LayerScans. This is done in the following way.
It is assumed that the physics TBB database is correct and functioning with the Run 2 LAr Electronics. The physics database does not need to and does not match the entries of the calibration database. For this reason it is not possible to transfer corrections tower by tower from the calibration database to the physics database and a prediction for the necessary change to the physics database is needed.
The required correction for each layer is measured and calculated for every tower individually based on the calibration TBB database with the help of the Phos4LayerScans. This is the precise correction which is inserted into the calibration database, see chapter 3. For the physics database this tower-wise correction is averaged over phi for every trigger tower with the same

eta resulting in, for example, 14 corrections for the A-side of the electromagnetic barrel (EMBA, $0 < \eta < 1.4$) for each layer.
The reason for this averaging is that it is tried to avoid over-correcting the physics database. A certain entry in the calibration database might be unusually far off from the optimal state and require a large correction. This layer of the trigger tower, however, might be better adjusted in the physics database and therefore not require the same amount of correction. Just transferring corrections from calibration to physics will therefore be dangerous.
The averaging is performed over phi since trigger towers in one eta slice are expected to behave similar due to the detector layout and structure of the front-end electronics.
This averaged correction is also validated by applying it to the calibration database and taking another set of Phos4LayerScans to avoid applying corrections with wrong signs to the physics database as well as ruling out major mistakes.
After this, the corrections for the Tower Builder Board delays for the physics database are eventually implemented.

## 2.6 PPM Input Timing

Inside the Level-1 Calorimeter system are the PreProcessor modules, described in section 2.2.7. With the PPM input timing, the time at which the trigger tower signals of one bunch crossing arrive can be synchronized for further components of the L1Calo Trigger. In this thesis it is used to adjust for the overall change in time of arrival of the full trigger tower signal between Run 2 and Run 3.
The PPM input timing difference to a previously chosen reference is always meassured as part of the automated online analysis and automatically done for the Phos4Scans. The resolution is 1ns and for calibration the input timing will be adjusted according to the results of this analysis.
Similar to the determination of the Tower Builder Board delays, it is more difficult to derive the input timing while taking data. Fortunately, no masking of the layers is needed and therefore the trigger remains working.
Measuring the input timing while taking data is also based on fitting functions according to established physics pulses acquired in Run 1 to the dig-

itized signals. The time of maximum amplitude is read out and compared to a previously chosen reference set. The deviation from that set is passed as a correction to the PPM input timing. This is done regularly at the start of a data taking period.
Nonetheless, it is preferable to start Run 3 with an approximate PPM input timing to ensure that early data is accurate and can be used. This also ensures that no additional resources are needed for the calibration of the PPM input timing for the Level-1 Calorimeter Trigger while taking data at the beginning of Run 3.
For the initial setting of the physics PPM input timing a prediction based on the change in electronics as well as the change in the Tower Builder Board database is used.
A schematic overview of the procedure to set the initial PPM input timing correction is shown in figure 2.7. The first major change in Run 3 that affects the PPM input timing are the newly installed LTDBs. These require the signals, necessary to build the Run 2 front- and middle-layer sums, to run through the LTDBs first before entering the Tower Builder Board. In contrast to that, the presampler and back-layer signals can enter the Tower Builder Board directly through the base plane. This is possible since the new Layer Sum Boards build the same sum for these two layers as in Run 2. This is expected by electronic experts to have the effect of delaying the front and middle layer by 8 or more nanoseconds with respect to the other layers (Private Communication, P. Schwemling-M. Wessels, 24.9.2019). Following

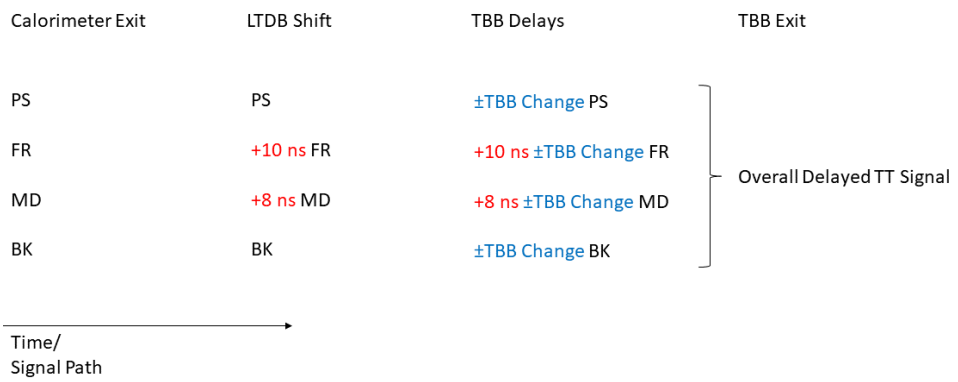


Figure 2.7: The graphic visualizes where the different time delays enter the signal path. The PPM input timing needs to account for the overall change after the TT signal leaves the TBB.

the signal, the next reason for a shift in PPM input timing in comparison to Run 2 are the new delays in the Tower Builder Boards. These can be positive or negative since it is also possible to reduce the delay of a specific layer for a trigger tower if that layer previously had a delay larger than zero. These are the two factors composing the correction for the PPM input timing. The first one, the electronics change, is not measured in physics. It is not required, since the pure electronics change is known and can be validated by comparing calibration runs before and after LTDB installation, see figure 3.2. Additionally, there is no reason to believe that the change is varying among the LTDBs.
The second factor contributing to the PPM input timing correction, the adjusted TBB delays, will be well-known and can be read out from the databases after adjustment are made. The electronics change and the TBB delay change added together are how the PPM input timing is proposed.

## 2.7 The Liquid Argon Phase-I Demonstrator

The so-called demonstrator region, between $0 < \eta < 1.4$ and $1.8 < \phi < 2.2$, is a region in the EMBA where pre-production versions of the LTDBs and further Phase-I Upgrade electronics have already been operated during Run 2. For this reason, there have already been adjustments to the Tower Builder Board delays and the PPM input timing. Section 3 will however show that a further adjustment is necessary for the production boards (replacing the demonstrator boards) and therefore the calculation of the PPM input timing and Tower Builder Boards will slightly vary for this region compared to regions equipped with LTDBs in LS 2. Due to this there are minor complications when treating this region since it requires smaller corrections.
In later plots it is sometimes the case that information from this region is excluded in the respective distributions to better highlight the symmetric structure of the histograms and keep the plot more readable. In these cases this will be explicitly mentioned.

# Chapter 3

# Tower Builder Board Calibration

In chapter 2.5 it was shown why new Tower Builder Board delays are needed. This chapter guides through the derivation and implementation of the new set of TBB delays. It also features necessary follow-up changes to the PPM input timing. Furthermore, the measurement accuracy of the presented procedure (see section 3.2) is examined.
During this thesis, the new LAr LTDBs in the A side of the electromagnetic barrel ($\eta < 1.4$) were fully equipped as part of the LS2 and delays could be determined.

## 3.1 Tower Builder Board Delays

### 3.1.1 Data Taking and Read-Out

The data used to derive the Tower Builder Board delays is generated by Phos4LayerScans. The data from the Phos4LayerScans is grouped by layer since one calibration run only tests one layer. The data is further grouped by which preprocessor crate the corresponding tower belongs to. The layers are always named by the channel of the trigger tower. This allows to identify to which trigger tower the layer calibration scans belong and only compare layers within one trigger tower.
The anaylsis consists of a first step to prevent misinterpreting the data. This is checking whether every layer inside the calorimeter has actually been pulsed with test signals like it should. During this test it was found

that inside the electromagnetic barrel there is a broken layer for one trigger tower in the Presampler, though this has been known before and was verified as broken cells. This can be seen in figure 3.1. It is a map of the Presampler in the EMB with positive $\eta$, the so called A-side, therefore also called EMBA. It can be seen that each TT layer in the Presampler gets pulsed as intended, marked as green, with the exception of the layer belonging to tower 0x00140803. The broken tower is highlighted in red and excluded from all further data processing in this thesis. There are no bad trigger towers on the C-side, barrel regions with negative $\eta$.

After verification of the recorded data being good, it is also first checked

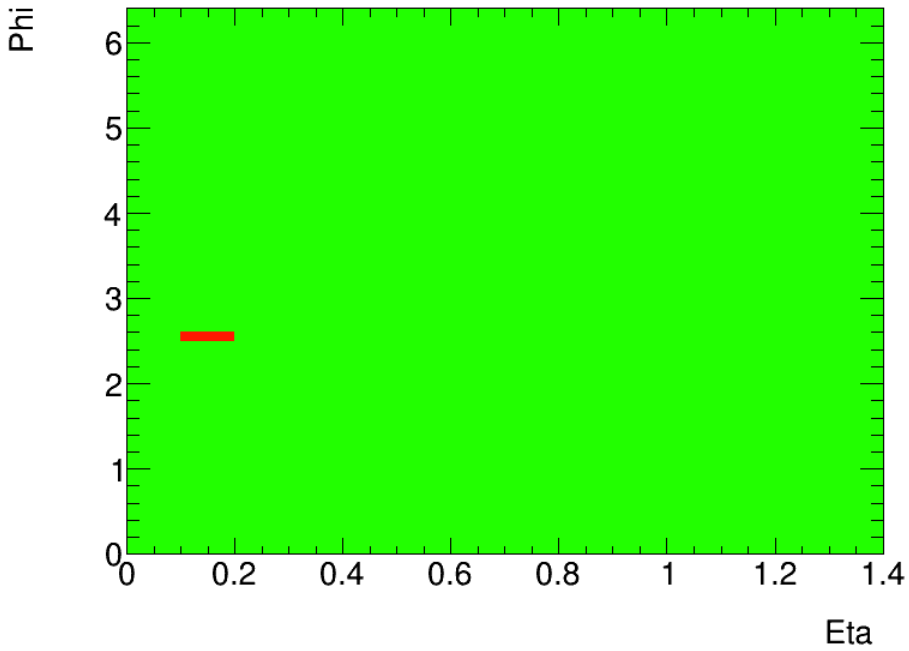


Figure 3.1: The EMBA, $0 < \eta < 1.4$, is shown. The colors code which trigger tower was available and working for the calibration. Green corresponds to working trigger tower, red marks bad towers.

whether the LTDBs influence the signal's travel time like they are expected to. This is done to rule out errors for later analysis and to confirm the system status. It was mentioned that experts from the Liquid Argon read-out electronics expect them to slow down the front and middle layer by about eight nanoseconds. For this, the system status directly before and after LTDB installation is compared. Therefore, the peak times of the signals for

all individual layers get calculated and the change read out. The result of how the signals shifted in time can be seen in figure 3.2. The figure displays

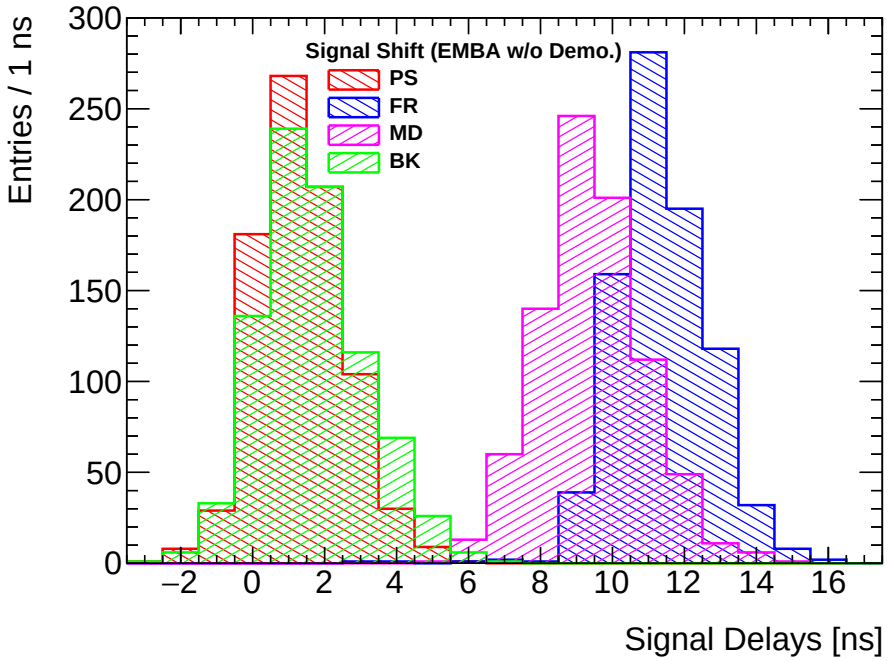


Figure 3.2: The time difference in signal travel time for the different layer due to LTDB installation is shown. The demonstrator region does not contribute to the histograms, only towers from the EMBA outside the demonstrator are considered.

by how many nanoseconds the signals are delayed after the LTDBs have been installed in comparison to before they were installed. It can be seen that the front and middle layer arrive significantly later. Concerning the middle layer it can be seen that the distribution made up of middle layers of all TT in the EMBA is centered around eight nanoseconds as expected. The front layer is also taking longer as expected, with even taking 2-3 ns longer than the middle layer. Overall the front layer takes ten to eleven nanoseconds longer after LTDB installation. The presampler and back layer do not change significantly. The figure shows a longer signal travel time of around one nanosecond for them. This is expected due to different routing of the signals through the baseplane. However, the impact of this minor change is small since the relative timing between the layers is restricted to multiples of 2.5 ns and is newly adjusted in the following. The overall width of the distributions can be assigned to measurement accuracy where more

details on this will follow in section 3.2. Overall, the expected behavior of the LTDB, regarding signal travel time, can be verified.
After verifying that the recorded calibration data is useful, the different layer calibration scans are compared using a peak finder method which writes out the peak time of the different layers. This means that it scans the entire signal and writes out the time corresponding to the maximum signal value. These peak times are compared to the peak time of the middle layer which has been chosen as a reference. This is done by simply subtracting the times when the calibration scans of the presampler, front and back layer reach their maximum value from the middle layer.
The basis for correcting the timing between the different layers in the EMBA is given by the five runs 375962 to 375966. These were taken in late February 2020. These are the first scans after the new LTDBs have been installed in the corresponding detector region. The results of these scans can be seen in figure 3.3.

The figure show the distribution of delays between the layers in nanosec-

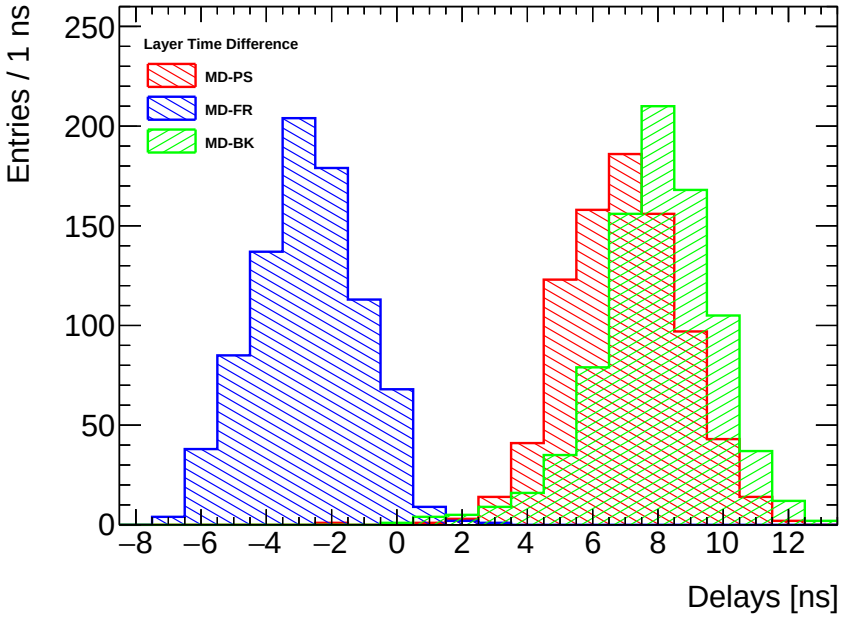


Figure 3.3: The figure, only representing time differences from the EMBA, features the distribution of delays between the different trigger tower layers with respect to the middle layer. The scans taken are from late February 2020 and are the first scans after successful installation of the LTDBs. The demonstrator is excluded from this plot.

onds. It can be seen that they deviate from zero in two groups. The Presampler and back layer signal arrive around seven to eight nanoseconds earlier than the middle layer. This is to be expected since the middle layer signals take the longer route through the new LTDBs which the Presampler and back layer do not. The time of eight nanoseconds which the longer route takes more is expected by Liquid Argon electronics experts (Private Communication, P. Schwemling-M. Wessels, 24.9.2019). The front layer signals also take the route through the LTDBs. It can be seen that these take around two nanoseconds longer than the middle layer for that.
These distributions are featured in other figures, in figures 3.4 to 3.6, later in this thesis once again as a reference colored blue. They deviate slightly from the ones in figure 3.3 due to the exclusion of the demonstrator. Therefore, later figures might have more entries around zero delay, since the demonstrator region has already been timed in Run 2.
Based on these first scans the goal is to introduce Tower Builder Board delays such that the layers will run in parallel again. Regarding the figure, this implies on trying to shift every distribution in a way where it is centered around zero. This happens in two different steps explained by the following two subsections 3.1.2 and 3.1.3.

### 3.1.2 Tower-by-Tower Corrections

For the first step the goal is to introduce delays individually for each layer in each trigger tower and correct with precisely the delay needed. This procedure is essentially shown in the previous figure 3.3. It is created by just filling each time difference between the different layer for every trigger tower into the histogram. Instead of just filling a histogram every delay for a trigger tower is written out and identified with the trigger towers COOLID. These delays needs to be introduced for the Presampler, front- and back layer so that they run in parallel with the Middle layer. Once more it should be noted that it is also possible to reduce the delay of the middle layer instead of increasing the delays of the Presampler and back layer. Further, it is to be noticed that the Tower Builder Boards cannot adjust the layer's timing with a resolution of one nanosecond but rather 2.5 nanoseconds. Therefore, the optimal delay gets rounded to the closest multiple of 2.5 nanoseconds.
Generally, when corrections are derived, they are further processed by experts from the Liquid Argon Calorimeter team, where the delays are opti-

mized in ticks to fit into the TBB database. This optimization, carried out by an algorithm, is necessary to make the best use out of the given range of possible corrections between zero and seven ticks. The algorithm also adds the corrections onto the existing Tower Builder Board delays in the database in the same step. The result of this approach was checked and can be seen in figures 3.4 to 3.6 below.

It can be seen that these individual corrections have centered the delays

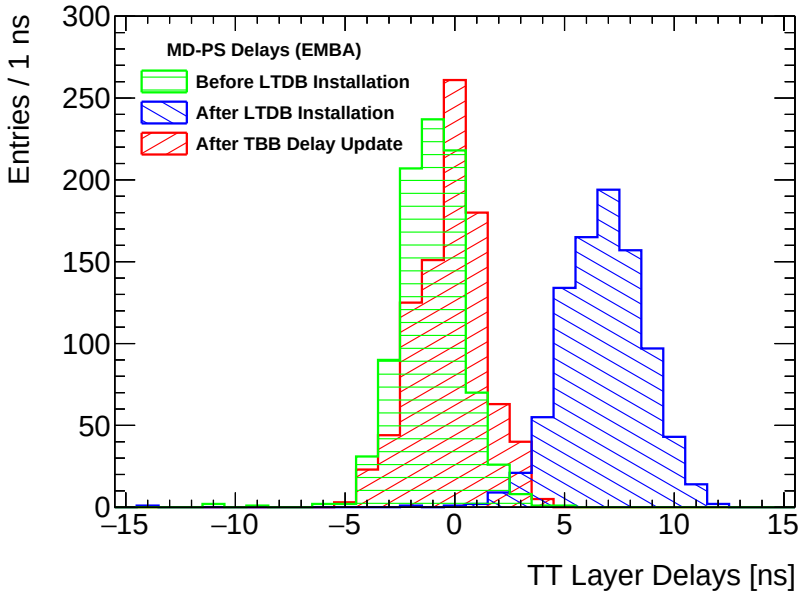


Figure 3.4: Shown are the delays in EMBA between the Middle layer and presampler after Tower Builder Board delay corrections have been introduced to the Tower Builder Board database. The blue curve shows the distribution without corrections as comparison.

between all layers around zero and the aimed for system status is reached. For better comparison, the distributions of the delays before correction and the distribution of the Run 2 status are presented as well. It is striking that the distributions of the delays feature a non-negligible width after the correction is applied.

The reasons for the distribution not being perfectly centered at zero are that corrections can not be implemented with arbitrary resolution. As mentioned before, corrections are limited to ticks of 2.5 nanoseconds, which itself creates a certain width of at least 1.25 nanoseconds. Essentially, at times the correction slightly over- or undershoot the precise amount of delay needed.

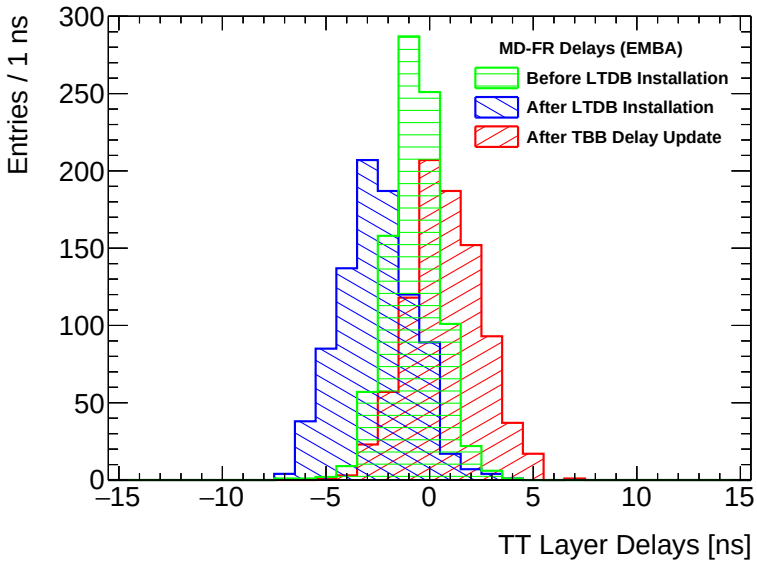


Figure 3.5: Shown are the delays in EMBA between the Middle and front layer after Tower Builder Board delay corrections have been introduced to the Tower Builder Board database. The blue curve shows the distribution without corrections as comparison.

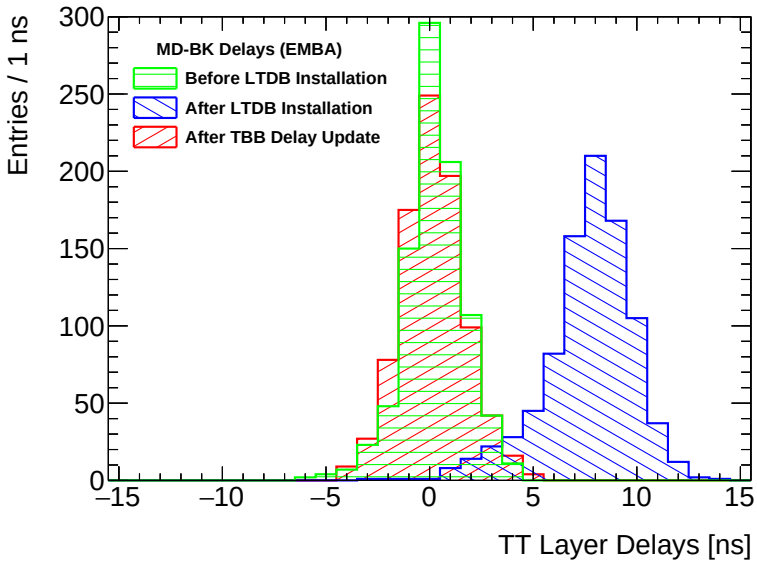


Figure 3.6: Shown are the delays in EMBA between the Middle and back layer after Tower Builder Board delay corrections have been introduced to the Tower Builder Board database. The blue curve shows the distribution without corrections as comparison.

A second reason is that corrections are not always applicable due to already far spread corrections in the Tower Builder Board database (delays are restricted to the range of 0 to 7 ticks). Though, this does not happen often, it will happen and simply cannot be avoided due to technical limitations. This fact, besides the natural width of the histograms, also can account for some delays remaining even larger than 2.5 ns between layers, where limitations are reached through the range of allowed ticks. A third reason for a not completely peaked distribution is the finite accuracy of the measurement. The measurement accuracy is about one nanosecond for individual scans of one trigger tower or layer and will be discussed in section 3.2.

### 3.1.3 Delays for Physics

In section 2.2.6 it is explained why the derived tower-by-tower corrections are not suitable for the set of delays in the database that is applied during physics data taking. However, they can be tuned such that it is also possible to correct the physics delays. For this they are averaged over phi, i.e. one average is build per eta bin (slice in eta of size 0.1). For the EMBA, an example of these averages can be seen in figure 3.7. It shows the averages

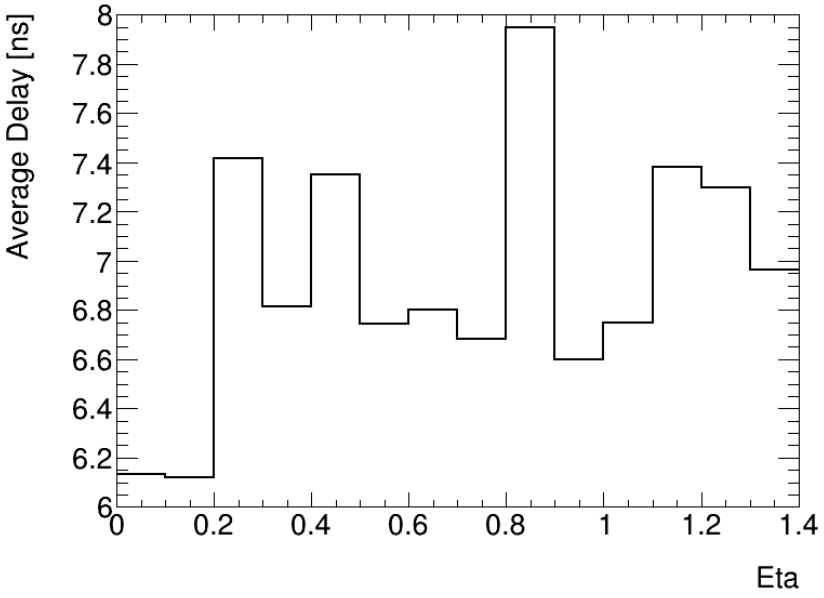


Figure 3.7: The distribution shows the average TBB delays in the Presampler which will be applied as corrections to the physics Tower Builder Board database.

built for the Presampler. It can be seen that with these averages all eta bins get 3 ticks as a correction since they are closest to 7.5 ns, except for the eta bins 0.0 and 0.1. These get 2 ticks as corrections as they are closer to 5 ns deviation from the middle layer. As previously, these averages in nanoseconds then get converted to ticks and implemented into the Tower Builder Board database. The results of these corrections can be seen in the figures 3.8-3.10. Though, these are corrections for physics it is still possible to test them on the calibration database to rule out major mistakes during the derivation. It can be seen that these distributions are centered around zero as well. However, they are slightly wider than the tower-by-tower corrections. This is expected to be like that since not every trigger tower has individually been taken care of. Instead, it was aimed to compensate the pure electronics induced shift by using the average delay as a correction. The derived corrections are suitable for data taking and are hence written into the physics database.

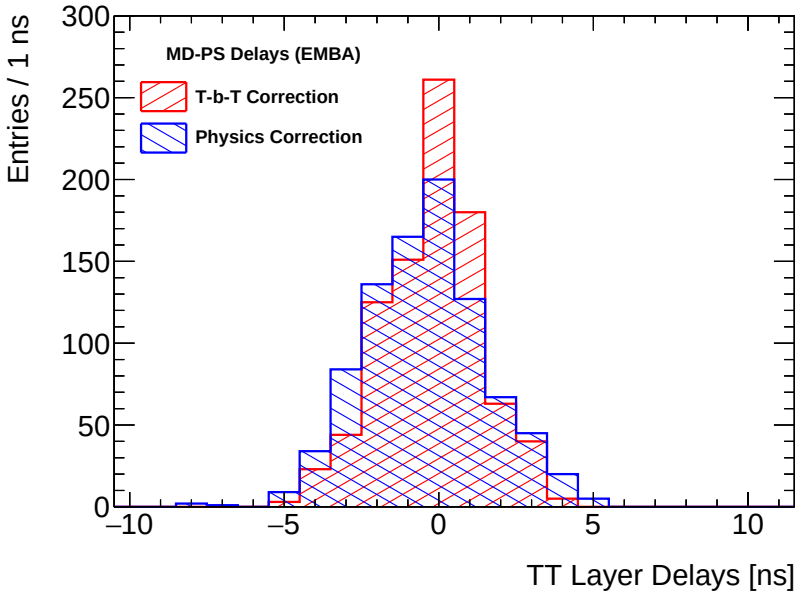


Figure 3.8: The distributions shows how the physics corrections (averages) to the TBB Database perform against the individual Tower-by-Tower corrections for the MD-PS delay.

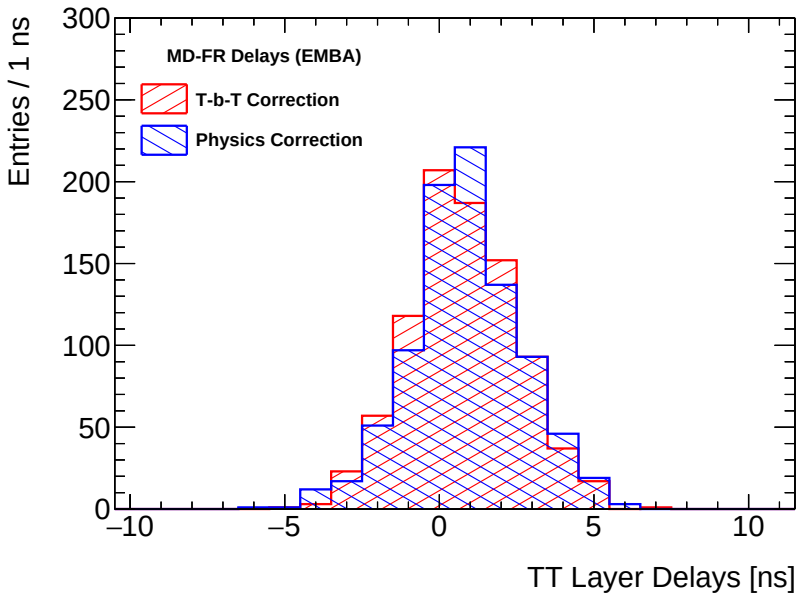


Figure 3.9: The distributions shows how the physics corrections (averages) to the TBB Database perform against the individual Tower-by-Tower corrections for the MD-FR delay.

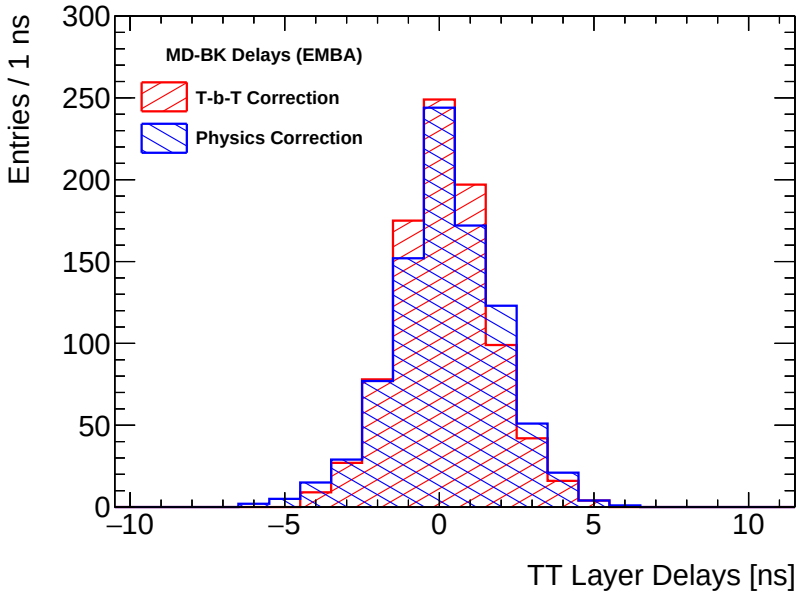


Figure 3.10: The distributions shows how the physics corrections (averages) to the TBB Database perform against the individual Tower-by-Tower corrections for the MD-BK delay.

| $\eta$ Bin | 0.0 | 0.1 | 0.2 | 0.3 | 0.4 | 0.5 | 0.6 |
|---|---|---|---|---|---|---|---|
| Correction PS | -2 | -2 | -3 | -3 | -3 | -3 | -3 |
| Correction FR | 1 | 2 | 1 | 1 | 1 | 1 | 1 |
| Correction BK | -3 | -3 | -4 | -3 | -4 | -4 | -4 |
| $\eta$ Bin | 0.7 | 0.8 | 0.9 | 1.0 | 1.1 | 1.2 | 1.3 |
| Correction PS | -3 | -3 | -3 | -3 | -3 | -3 | -3 |
| Correction FR | 2 | 1 | 1 | 1 | 1 | 1 | 0 |
| Correction BK | -3 | -3 | -3 | -3 | -3 | -3 | -2 |

Table 3.1: The derived averages for TBB delays in the EMBA which will be deployed as corrections to the physics TBB database are shown in ticks. The ticks are always with respect to the middle layer. The middle layer does therefore not experience a change in this representation.

| $\eta$ Bin | 0.0 | 0.1 | 0.2 | 0.3 | 0.4 | 0.5 | 0.6 |
|---|---|---|---|---|---|---|---|
| Correction PS | -2 | -2 | -2 | -2 | -2 | -2 | -2 |
| Correction FR | -1 | 0 | 0 | 0 | -1 | 1 | 0 |
| Correction BK | -1 | -1 | -2 | -2 | -1 | -2 | -2 |
| $\eta$ Bin | 0.7 | 0.8 | 0.9 | 1.0 | 1.1 | 1.2 | 1.3 |
| Correction PS | -2 | -2 | -1 | -2 | -2 | -1 | -2 |
| Correction FR | 1 | 0 | 0 | 0 | 0 | 0 | 0 |
| Correction BK | -1 | -2 | -1 | -2 | -2 | -1 | 0 |

Table 3.2: The derived averages for TBB delays for the demonstrator region are shown. They are presented analogous to table 3.1.

The physics set of corrections for the TBB delays in the EMBA is represented by table 3.1. The table shows ticks, multiples of 2.5 ns, as corrections. These are based on the middle layer remaining unchanged. The middle layer would therefore have only zeros as entries in this table. Keep in mind that this will not necessarily be the absolute correction received by the database since an algorithm will optimize it and shift the ticks around while keeping the correct differences between the layers.
Since the demonstrator underwent adjustments during Run 2 the corrections necessary are smaller. Table 3.2 shows these in the same way they are presented for the rest of EMBA.

## 3.2 Measurement Accuracy

In the following, the measurement accuracy of the determination of the delays is discussed. For this three different Phos4LayerScans at two non consecutive days have been taken. For these the time differences between the middle layer to the presampler, front- and back layer have been calculated. After calculating these for every tower in the EMBA they have been subtracted from the results obtained in the other Phos4LayerScans. Figure 3.11 shows how often a repeated Phos4LayerScan is likely to produce the same result as a previous one. The accuracy (standard deviation of 3.11) of determining a delay therefore is one nanosecond.

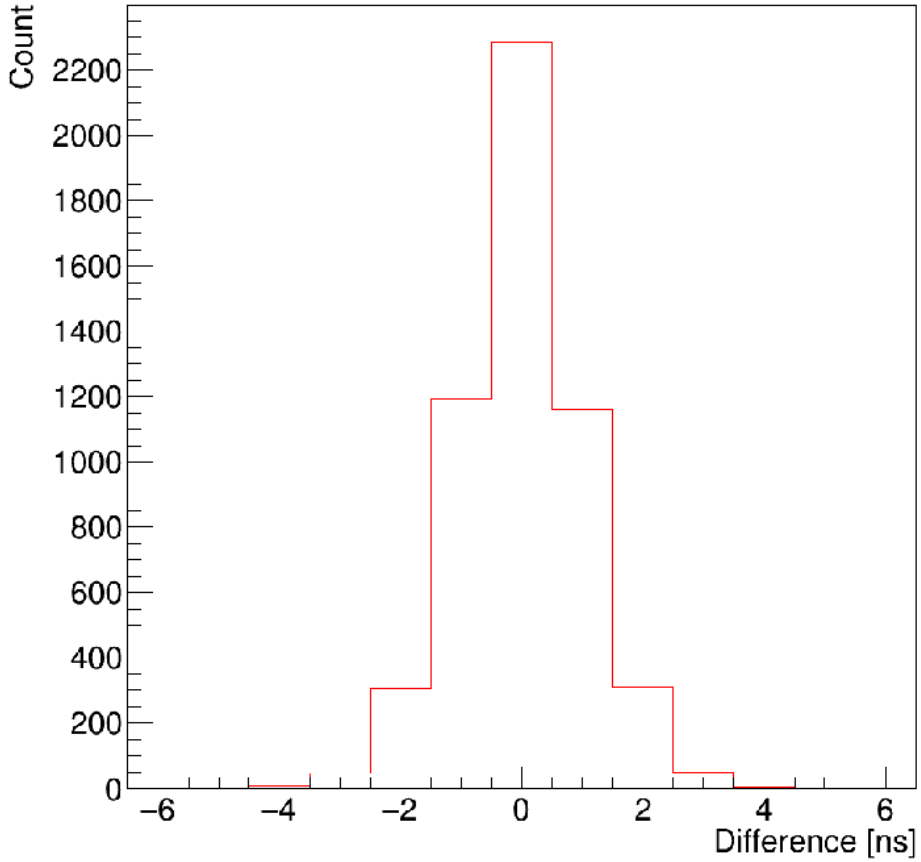


Figure 3.11: Shown is the discrepancy of the delay estimation (between the middle layer and the other layers of the electromagnetic calorimeter) for repeated measurements of the same delays using all TTs in the EMBA for three Phos4LayerScans.

The reason why the delays are compared and not for example peak times is that this measurement then also includes the uncertainties introduced by the general method to derive the delays and peak finder used to calculate the delays.
It has already been mentioned that the method chosen to find the peak time of the signal is a peak finder. There have also been studies on whether a forward going peak finder (a peak finder sampling the maximum amplitude from left to right) will always yield the same result as a backwards searching peak finder. For signals with a broad peak or low resolution in signal amplitude it can occur that these two will not choose the same peak time depending on how they are implemented. The following overview however shows that this is not the case for the signals used in the layer scans since they always have a high enough resolution in signal amplitude to uniquely identify the peak time. This can be seen in figure 3.12 which shows the difference in time the two peak finder variants yield. The time difference was calculated by comparing the two peak finder for the layer tuns 375962, 375963 and 375966 for every TT in the EMBA. The similarity of the results of the peakfinder methods were validated for 2688 pulsed layers of different TTs, where only for 5 pulses different peak times were found. This shows that the simple forward going peak finder is precise enough to be used for the purpose presented.

### Fit Performance

The peak finder is only limited to the step size the Phos4LayerScans have in time. Therefore it is restricted to a one nanosecond resolution. To be able to acquire higher resolutions for the peak time there has been the idea of using established fitting functions for the Phos4Scans and use the peak time the fit yields as a parameter. The functions are described in [10] and essentially are a gaussian for the rising side and a gaussian or landau function (depending on detector region) on the falling side.
This procedure has been tested, but was ruled out because the desired resolution of one nanosecond or below could not be achieved. The fitting functions worked, however not to a precision close to the one desired. The fit functions did not perfectly describe the layer scans. This might have multiple reasons like a minor change in shape from Run 1 to 3 or more likely that the

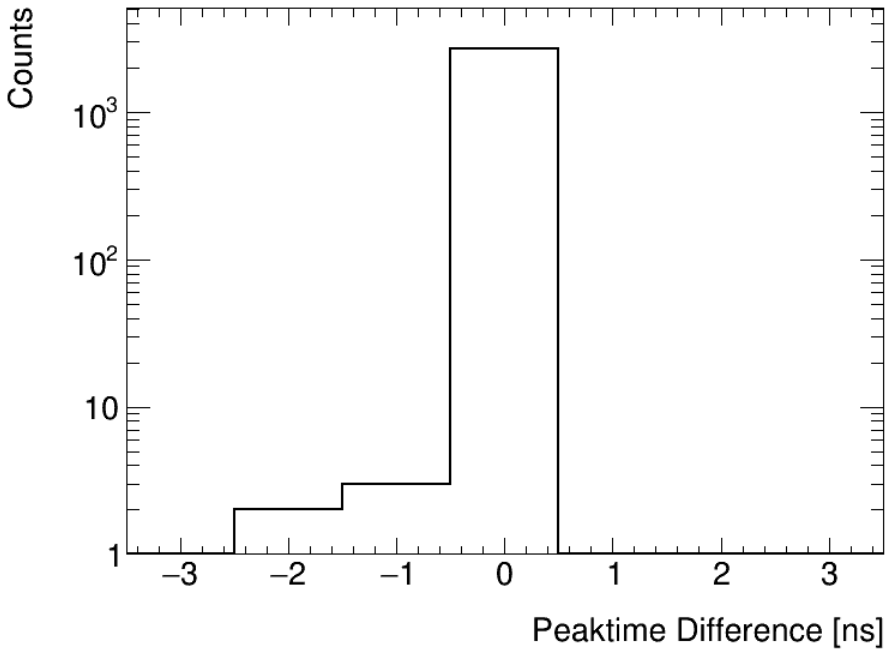


Figure 3.12: Shown are how often the peak times from the forward and backwards going peak finder deviate from one another.

function was originally designed for full tower signals and not layer signals. We know that layer signals might vary slightly from one another, therefore it would not be surprising if the full tower function does not fit the layer signal. Another reason which made pursuing this possibility less attractive is that due to the Tower Builder Boards using ticks as a correction, a resolution of the needed delay below one nanosecond would not have improved the results significantly. These reasons lead to the peak finder being the method of choice to finding peak times.

## 3.3 PPM Input Timing

As described in section 2.6, changes in the front-end electronics affecting the signal path and signal travel time lead to a necessary adjustment inside the Level-1 Calorimeter system. There it is necessary that the signals are synchronized and to know when exactly they are arriving.
For calibration scans this can easily be measured and is always done by comparing the current time of arrival inside the Level-1 Calorimeter system

with a saved reference from Run 2. Examples for such an automated measurement can be seen in figure 3.13. This difference then is implemented into the PPMs to calibrate them.
For physics this can not be done this easy, due to the complications presented in section 2.6. Therefore, a correction for the PPM input timing needs to be implemented before continuing to take data in Run 3 and to ensure a smooth start. In fact, during physic runs the PPM input timing will be monitored and always readjusted if necessary. For the correction of input timing before runs start again it is important that the Tower Builder Board delay changes have already been implemented. Once these are implemented and confirmed it is possible to download the database which is in place and compare it to the database of the Run 2 settings. Having these two, the difference between them is calculated and noted as the 'software' change to the signal travel time. For the hardware induced change, regarding the signal time, the mean of the distributions in figure 3.2 is taken. These exactly reflect how much later the different layers arrive. Since the change is uniform for the entire EMB it is not necessary to take local variations into account.
These two components are added up into the final correction for the PPM Input Timing. Deriving the correction for physics is not possible yet since the TBB delay corrections to the TBB database will only be implemented for all detector parts at once when they are finished.
To still check the functionality of this procedure there has been a test to predict the PPM input timing correction necessary for calibration and compare it to the automated analysis. It is useful to test the prediction of the PPM input timing for calibration since here, another analysis is available and the results can be compared and validated. For physics there is no such possibility and the prediction needs to be trusted. The comparison is shown in figure 3.13. It can be seen that the important features, like the central dark blue ridge around $0.5 < \eta < 0.7$ where a lower correction of -1 and -2 nanoseconds is needed, do overlap. It can also be seen that in large regions of the detector a correction of +1.5 nanosecond is necessary. Both ways of deriving the input timing correction come to the same conclusion on this. One last thing to mention concerning the PPM input timing is that in these comparisons, between predictions and measurements for calibration runs, the prediction seems to have a lower resolution in time than the mea-

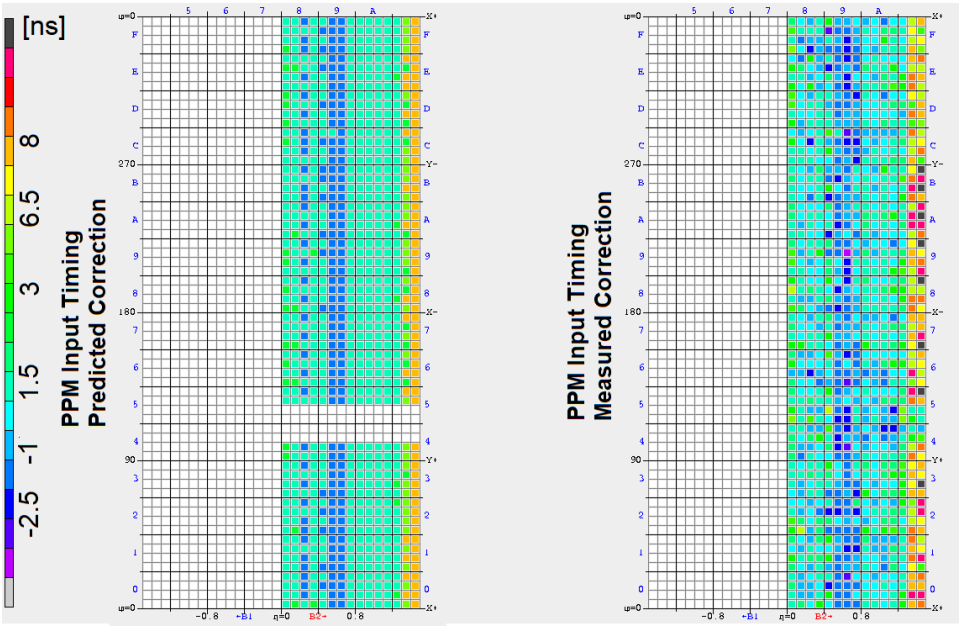


Figure 3.13: The two $\eta$-$\phi$ maps show the correction necessary to the PPM Input Timing for the calibration setup. The left side shows the derived/predicted prediction. The right side presents the automated results from the online analysis.

surement. This is in fact true since the prediction is based on changes in the Tower Builder Board database. Therefore it is subject to the resolution limitation of the TBB database which is 2.5 nanoseconds. Furthermore, the demonstrator has been taken out of the prediction since it was influenced by multiple corrections for Run 2 and the LTDB installation in the demonstrator back then. The prediction however is made for most parts of the detector where LTDBs and corresponding corrections have not been in place in Run 2.

# Chapter 4

# Pulse Shapes

After investigation and calibration of the Tower Builder Board delays it is crucial to verify that there are no unwanted changes introduced to the full trigger tower signal. Chapter 4 will focus on the signal shape, represented through the signal rise time as well as signal height.
The studies from this chapter can not be performed on further parts of the detector, besides the EMBA, at this point in time. These studies only make sense to perform on regions of the detector once the Tower Builder Board delays for calibration runs have been set which is not the case, for all parts besides the EMBA, at the time of writing of this thesis.

## 4.1 Rise Time Changes

An important difference to previous chapters is that from now on the signals used are not generated through Phos4LayerScans anymore, but usual Phos4Scans. With these it is now possible to receive full trigger tower signals, i.e. signals which are made of the TBB sums of all four layers in the electromagnetic calorimeter. The resolution of Phos4Scans is still one nanosecond. The analysis of the full trigger tower signal is only possible once the TBB delays have been set.
The first quantity to be investigated towards possible changes of the signal pulse is the rise time of the signal. It is defined as the time difference between the signal reaching 10% and 90% of its maximum signal height. For regions in the electromagnetic barrel, values around 35-45 ns are expected, compare figure 4.2a. The rise time together with an example for a signal

generated through a full tower Phos4Scan can be seen in figure 4.1.

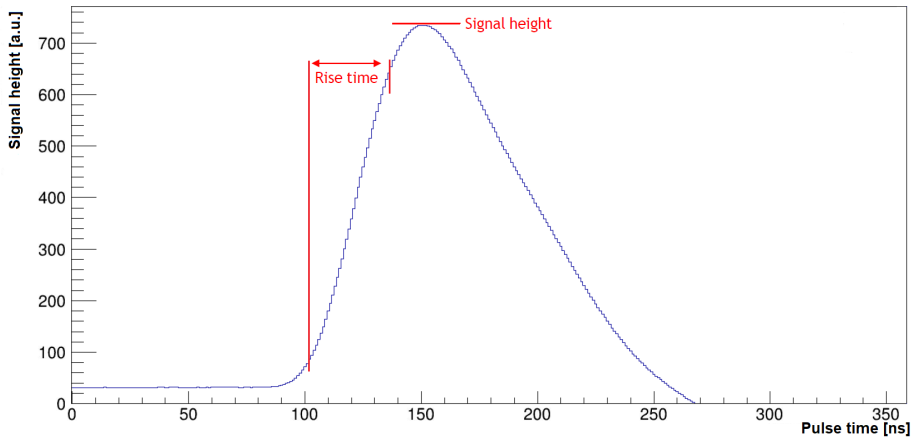


Figure 4.1: The definition for rise time and signal height is visualized together with an example for a Phos4Scan (after LTDB installation) for a full trigger tower in the EMBA.

The distribution of the rise time across the EMBA for Run 2 has been measured and is shown in figure 4.2a. Rise times have also been calculated for new Phos4Scans taken after LTDB and Phase-I Upgrade electronics have been installed, see figure 4.2b, to properly compare the new rise times to previous ones from Run 2 and extract how the rise time shifted. It was mentioned before that the demonstrator region was already equipped with LTDBs in Run 2. Possible changes of the rise time should thus be detectable by comparing the measured rise time in the demonstrator region to the rest of the EMBA. It can be seen in figure 4.2a that the rise time does not show a different behavior in the demonstrator and therefore no major change is expected in Run 3.
Using the $\eta - \phi$ maps it can be seen that the distribution of the rise time has not systematically changed along eta or phi. The pattern remains the same which can be seen when subtracting the two maps from one another. In that case it results in a uniform distribution confirming no significant change, this can be seen in figure 4.2c.
To interpret possible overall changes it is easier to take a look at the distribution of the individual rise times in figure 4.3. The blue distribution shows the rise times present before LTDB installation after Run 2 and the red distribution features the rise times with Phase-I electronics in place. It shows that the distributions match each other, i.e. their general shape is

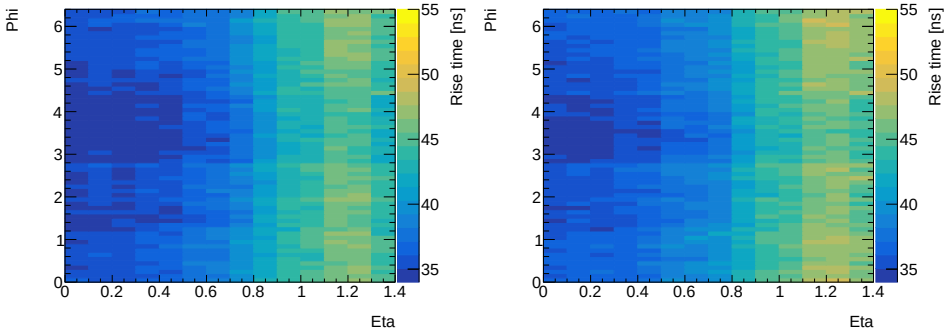


(a) before LTDB installation




(b) after LTDB installation

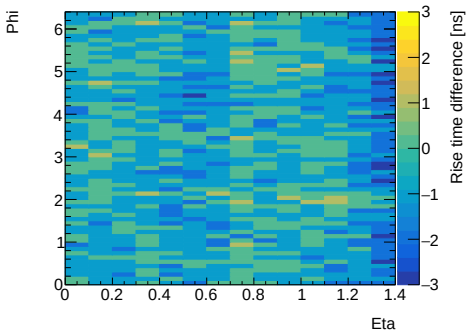


(c) Difference Run 2 and Run 3

Figure 4.2: The $\eta$-$\phi$ maps show the rise time in Run 2 (a) and Run 3 (b) as well as their difference (c). No functional change can be seen between Run 2 and Run 3.

similar and no unusual outliers are found. However, the new rise times are slightly shifted towards larger values by approximately one nanosecond.
As will be explained in section 4.1.1, the rise time plays a significant role for the Level-1 Calorimeter Trigger. Since the shift is minor it is hard to locate where it originates from. It might be that the rise time truly has not changed and that the shift is due to the measurement accuracy for single trigger towers. The measured accuracy of a delay found by the peak finder algorithm derived in section 3.2 is still comparable for the full tower Phos4Scans presented here. However, to derive a rise time the calculation needs points in time which are located on a steep section of the signal of the Phos4Scan. Due to the two points, needed to calculate the rise time, lying on steeper parts of the signal, the change in amplitude one nanoseconds makes is larger. The resolution of one nanosecond in time therefore enforces compromises when choosing the time stamp where the signal hits 10% and

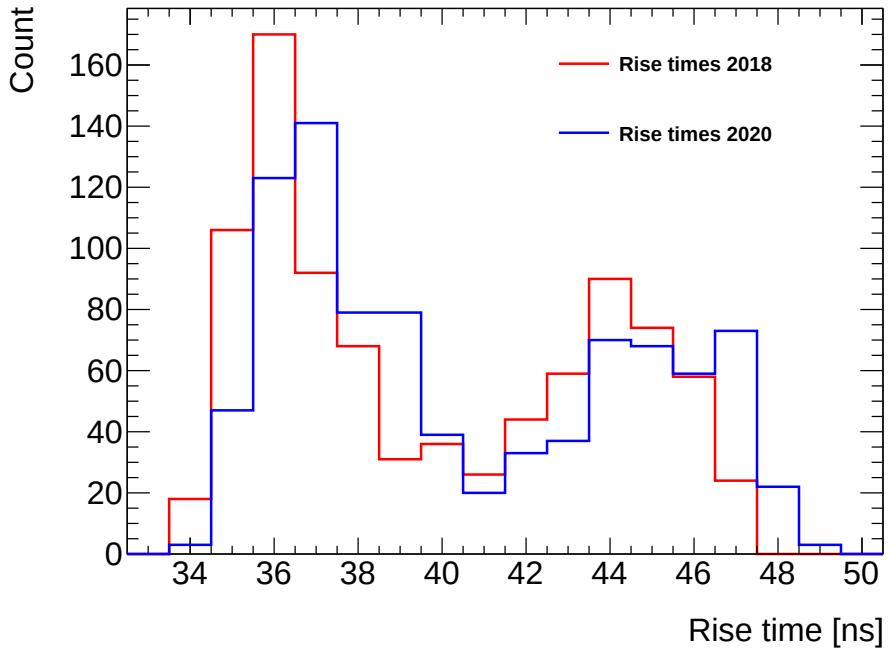


Figure 4.3: Comparison of the rise time distributions before LTDB installation (red) to after LTDB installation (blue).

90% of its maximum height. This effect also plays a role and can lead to minor differences in the rise time between Run 2 and the Phos4Scans now. Since it cannot be ruled out that there is a systematic change, not originating from measurement inaccuracy, it will be beneficial to check whether this small change would have an influence on triggering.

### 4.1.1 Effects on Trigger Performance

Changes in rise time play an indirect role in the bunch crossing identification of saturated signals in real time. If the signals saturate there is an algorithm in place, called Sat80 [11]. It identifies (using 80Mhz sampling) which one of the digitized saturated points originates from the maximum value, to correctly assign the signal to the bunch crossing it comes from. The algorithm uses the last three points before the signal saturates as input. These are then compared to two thresholds, called high and low. Based on whether each of the three samples has energy lower, in between or higher than the two thresholds a decision is made which sample after saturation corresponds to the original bunch crossing. The rise time effects this since a larger rise

time results in higher values of the signal for the same distance (in time) from the maximum than previously. If this effect is significant, it would require a change of the thresholds.
Following the logic for choosing the thresholds in [11], the minor change in rise time would not lead to a significant change of thresholds for the EMBA, as these would only change by a few ADC-Counts. The new thresholds would still be well within the range from which the Run 2 thresholds have been chosen and therefore no impact on the performance of the trigger is expected.

## 4.2 Pulse Height

Another signal property to be examined is the signal height of the test signal. Ultimately, it is the height of the signals generated by particles which is directly proportional to the deposited energy in the trigger tower. Changes due to new electronic parts regarding the amplitude are therefore important to understand so that they can be taken into account properly.
For this, all the signal heights for two Phos4Scans, one before LTDB installation and one after, are read out. The signal height after LTDB installation is subtracted from the one in Run 2 and can be seen in a $\eta$-$\phi$ map of the EMBA in figure 4.4. Comparing the difference in signal height for the demonstrator region with the remaining trigger towers in the electromagnetic barrel, a distinct pattern is observed. It does not show any difference in amplitude while the rest of the EMBA does. This is expected since there have already been LTDBs in place during Run 2 and therefore no change should be visible. Minor deviations from zero can be explained by switching from demonstrator or pre-production boards to the actual LTDBs used in Run 3. The change in amplitude can be further investigated in figure 4.5. It features the distribution of the signal heights before (blue) and after (red) LTDB installation. An approximate decrease of 5% of the signal amplitude is observed. This is expected from the design of the new electronics (Private Communication, P. Schwemling-M. Wessels, 19.9.2019) and can be confirmed here.
The limitation of the Phos4Scans is that the signals are always injected with the same energy. While the amplitude behavior is as expected, it is necessary to check this for the entire energy range and look for unexpected behavior. This is shown in chapter 5.

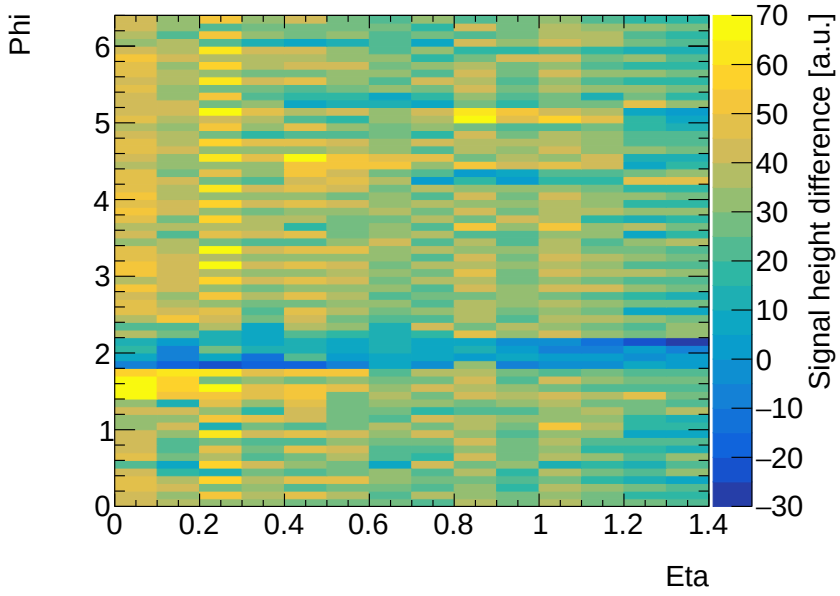


Figure 4.4: The $\eta$-$\phi$ map shows how the difference in signal amplitude between Run 2 and Run 3 varies across the EMBA. The demonstrator region can be seen for $\phi$ values in between 1.8 and 2.2. There, LTDBs were already installed in Run 2 therefore no change with respect to the Run 2 configuration is expected.

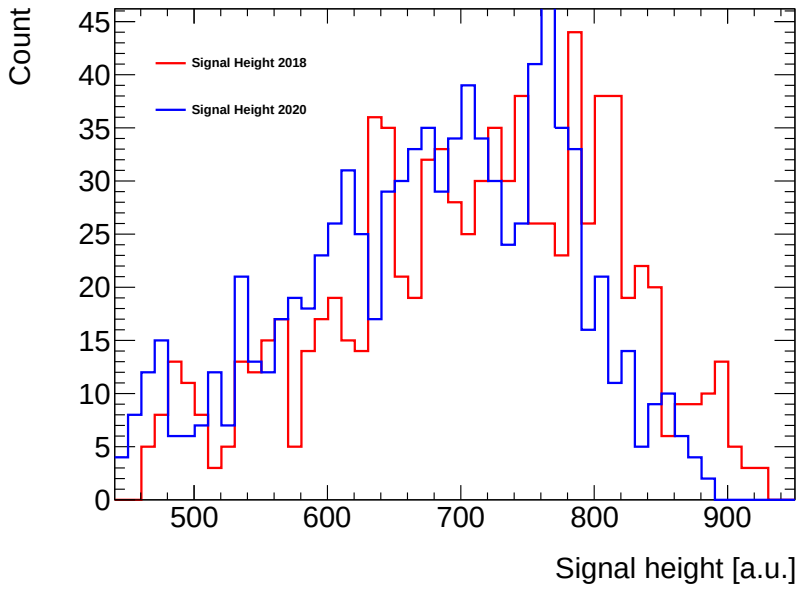


Figure 4.5: The two distributions show the signal heights for all trigger towers in the EMBA for Run 2 (red) and after LTDB installation (blue). The distribution for the signal height after LTDB installation is shifted towards lower amplitudes by approximately 5%.

# Chapter 5

# Energy Calibration

The last chapter of this thesis covers the topic on how the loss in signal height, seen in chapter 4.2, continuous at different input energies. For this the various factors composing the energy read-out are shown and so called energy ramps are analyzed.

## 5.1 Energy Ramps

To be able to accurately determine the signals attribute of interest a high resolution in time has been required in previous chapters. For the signal height and the energy it represents this is not necessary. Therefore, the procedure to create signals used in the following will not use Phos4Scans but rather a procedure covering multiple energies. The signals are digitized every 12.5 nanoseconds while the read-out is adjusted in a way making sure one digitization point is always aligned with the highest signal value. To cover a wider range of energies each tower is pulsed with each increasing energy 200 times. The energy, read out by the L1Calo systems, will then be compared with the energy that should be measured, which is the input. For so-called short energy ramps it is made sure that the input energies start from shortly above the noise threshold and increase up to the ADC saturation level of 1023 ADC-counts (corresponding to 255 GeV with a 8 bit resolution of the ADC). For long energy ramps the energies fed into the system reach far above that point up to an equivalent of close to 5 TeV. Long energy ramps can for example be used to study the saturation behavior of the signal.

### 5.1.1 Short Energy Ramps

Short energy ramps are perfectly suited to investigate the previously seen loss in signal height. An example of how a short energy ramp for one trigger tower looks like can be seen in figure 5.1. The figure shows the multiple in-

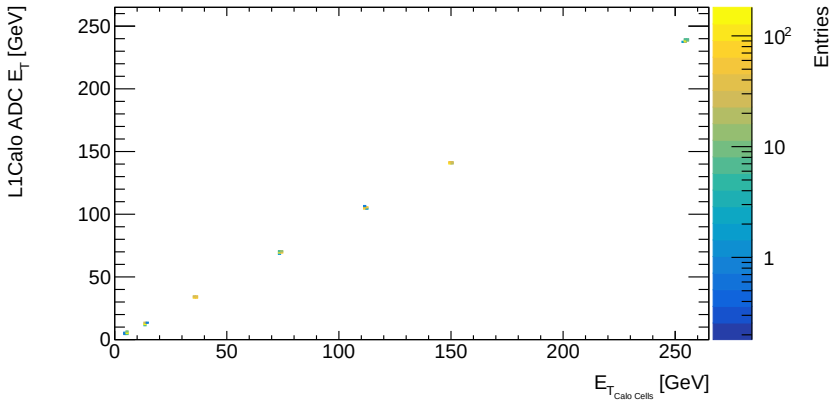


Figure 5.1: Shown is the read-out of a short energy ramp for a single trigger tower, tower 0x0100e00. The L1Calo energies of the TT are pedestal corrected by 8 GeV.

jections at various energies. The energy injected is displayed on the x-axis as Liquid Argon energy and the energy received by the L1Calo Trigger system composes the y-axis. If the aforementioned loss in signal height continues to all energies this should be visible by a slope smaller than one when fitting a linear function through these points. Fitting a linear function is done for all trigger tower in EMBA and the slope is read out and showcased in figure 5.2. The figures shows the results for the slope parameter of the fit. It can be seen that everywhere, except for the demonstrator, the slope is below one. Errors are not shown in the figure but they are strictly small enough so that the difference between the demonstrator and the rest of the EMBA is significant. Therefore, it can be concluded that the expected loss in signal height transfers linearly to all energies. This imposes no problem towards Run 3 as this can be resolved by adjusting the gains in the L1Calo receivers.

Gain factors are essentially a factor of amplification, for the signal coming from the detector to the L1Calo trigger system, to accurately calibrate the signal strength/height so that it matches the scale the L1Calo system expects and is working with. In this case, gains allow for the possibility to

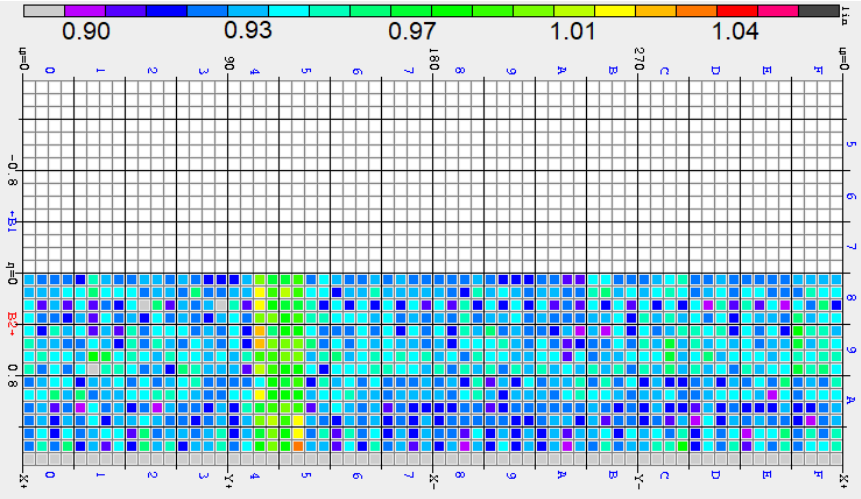


Figure 5.2: The slopes of the linear fits through the short energy ramps in the EMBA are shown on the $\eta$-$\phi$ map. Note the figure is rotated by 90° degrees to the right.

increase the signals amplitude from Run 3 back to the same standard as in Run 2, since the Run 2 level is expected by the system. This has happened for the demonstrator in Run 2 and can be seen in figure 5.2 as well. The demonstrator boards installed in Run 2 and the production LTDBs do not vary from another too much so that the adjusted gain ensuring a correct energy correlation, i.e. a slope of 1, is visible here.

Figure 5.2 does not allow for a general validation of working energy correlation between the Liquid Argon read-out and the L1Calo read-out. Individual trigger towers might have a correct energy correlation but a wrong offset. This can be seen by either checking for the offset, the second fit parameter, directly or displaying all trigger towers at once. Displaying all trigger towers at once is less exact regarding the offset, however also allows to spot other unusual behavior and outliers. An example for a trigger tower with wrong offset can be seen in figure 5.3 where an outlier is visible. The figure shows a short energy ramp for all trigger towers in the EMBA (the offset of 8 GeV is due to a pedestal value of 32 ADC-Counts underlying the signals, also visible in the Phos4Scans, compare figure 2.6). One trigger tower which is shifted to lower L1Calo energies can be spotted. This trigger tower is also visible when directly checking the offset for the linear functions fitted through all trigger towers individually. The search for the exact issue of

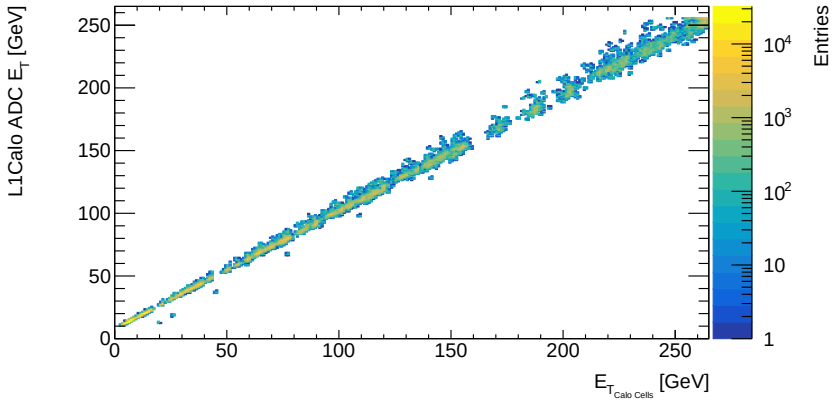


Figure 5.3: The short energy ramp read-out from all TT in the EMBA is shown. One trigger tower has a bad energy offset and is seen seperated below (note that one TT has 200 injections at each energy).

energy miss-alignment is still going on at the time of writing. However, it is only a single trigger tower and no conceptual errors can be seen.

### 5.1.2 Long Energy Ramps

Long energy ramps are used to study the saturation behavior of the signals. It is checked whether the signal peak runs into saturation linearly or if there is a loss of signal height/energy close to saturation. The last point before reaching saturation is therefore important. It needs to be checked whether the signals height gets cut slightly when digitizing the signal at that point. To investigate this, linear functions will again be fitted to the the energy ramp up to (including) the last point not saturated. Furthermore, the fit is performed again but excludes the last point before saturation. If the last point would suffer a drop in signal height it would therefore lower the slope and differences in slope between the two fits could be detected. The result of this procedure is visible in 5.4. It is an $\eta$-$\phi$ map showing the difference in slope between the two fits. It can be seen that the difference is very low and approximately uniform. Minor differences are accounted for by the limited precision of the injections. To put the values of the differences into perspective a reference has been created. If the last point before saturation were to drop one percent (or 10 ADC Counts) it would present itself in a difference in slope of at least 0.05 and extremely worse fitting accuracy and Chi-Squared values. Neither were observed during the investigations.

The obvious outliers in figure 5.4, being dark blue or grey, are due to the last injection being exactly at the border of saturation. In that case, a part of the 200 injections at that energy are above saturation and the other part below. This leads to a smearing of that point and worsens the fit. All outliers have been checked with respect to this and they all were identified with the last injection being partially saturated.
It can therefore be seen that the values for the differences between the fits measured are below values indicating significant change and systematic changes regarding saturation behavior can be excluded.

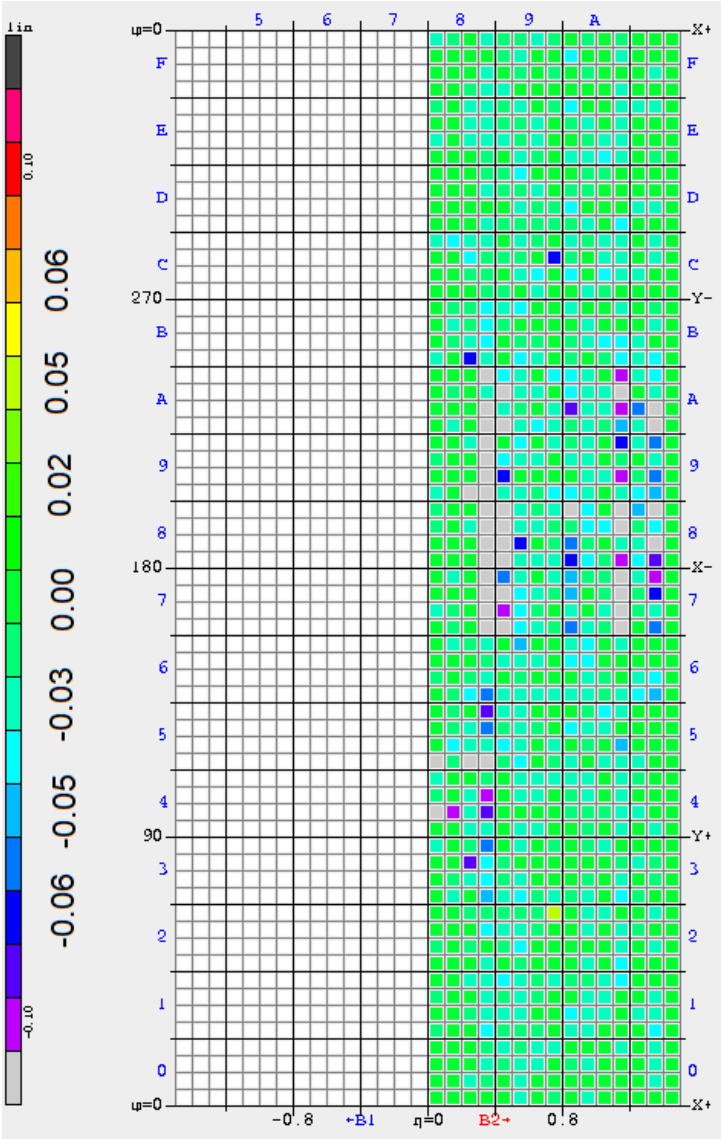


Figure 5.4: The difference in slope when fitting with and without the last point before saturation can be seen. Close to no change shows normal saturation behavior in the EMBA.

# Conclusion and Outlook

Efficient triggering and event selection is a central concept for experiments at the Large Hadron Collider due to the enormous collision rates. To allow for a fast first selection of events at the ATLAS experiment, the Level-1 Calorimeter Trigger is working with reduced spatial information. The information is reduced by electronic hardware elements, mounted directly on the detector, before passing the signals to the Level-1 Calorimeter Trigger which evaluates the data coming from the calorimeters. Due to collisions occuring every 25 nanoseconds, precise knowledge of all the different electronic components and their individual latency is needed.
During the present Phase-I Upgrade of the Level-1 Calorimeter Trigger and electronic components involved, new electronics are installed to allow for a finer spatial resolution of the energy deposition in the first level of triggering. This is necessary to maintain a reasonable event rate at the higher expected luminosity of Run 3 without increasing the trigger thresholds significantly where possible. Parallel to the new trigger system installed, the Run 2 system will be kept as a well-understood backup in Run 3 and experiences new time shifts for the different layer signals of the electromagnetic calorimeter. The measurements and the readjustments of this shift are the first part of this thesis. The time delay is identified to be around 8 nanoseconds for the middle layer and around 11 nanoseconds for the front layer of the electromagnetic calorimeter. The Presampler and the back layer remain unchanged up to minor differences of 1 nanosecond. This small shift can be attributed to slightly different routing of the signal as well as the measurement accuracy. The shifts between the layers are converted into a correction for the Tower Builder Board database so that the layer signals can again be summed up correctly at the maximum signal height into one full Trigger Tower signal. The functionality of the updated configuration of the

Tower Builder Board delays is confirmed using special Phos4Scans. Within the possibility of running the new Tower Builder Board delays for physics in Phos4Scans they are also confirmed as working and can be immediately utilized when data taking in Run 3 starts.
As a consequence of the electronic changes and the new Tower Builder Board delays, studies are performed to predict the time-wise shift needed for the the input timing correction of the PPMs of the L1Calo Trigger system. The input timing is derived for the calibration database using Phos4Scans and compared to the results of the automated analysis that is performed for each scan. Differences of the input timing are observed for the demonstrator region. The differences are due to the fact that the demonstrator has already experienced adjustments of the PPM input timing in Run 2 and therefore making it hard to trace all of them back accurately. Studies concerning this issue are still ongoing. With this one exception, the PPM input timing prediction for physics is reliable and can be applied to further parts of the detector outside the EMBA.
Besides the timing studies, additional signal properties are investigated. This includes a comparison of the signal rise time between the Run 2 and Run 3 system, where small changes of approximately one nanosecond are observed. Investigation of this shift and its effect on the bunch crossing identification of saturated signals will continue in the future. Comparisons with the EMBC will also bring further insight onto whether an actual change in rise time is taking place or if it is measurement accuracy related.
Furthermore, the signal amplitude is analyzed and a decrease of around 5% is visible in comparison to Run 2. This was an expected side effect of new electronic components and can be treated with adjustments of the gain for physics runs.
Future work will see the completion of LTDB installation outside the EMBA and consequently the important adjustment of Tower Builder Board Delays for the remaining calorimeter. In addition, the timing and signal property studies presented in this work, like the determination of the PPM input timing, need to be done for all other parts of the detector receiving new LTDBs and their behavior needs to be analyzed. It is expected that the behavior of other regions is comparable to the EMBA such that methods developed in this work can be applied to further regions of the detector and necessary changes can be extracted and implemented.

# Appendix A

# EMBC Time Differences

The following figures A.1-A.3 present preliminary results for the time differences between trigger tower layers in the EMBC. 13 out of 16 Crates (728 of 896 TT) containing Phase-I Upgrade electronics have been installed at the time of writing. The delays due to LTDBs in the EMBC agree with those from the EMBA observed after LTDB installation.

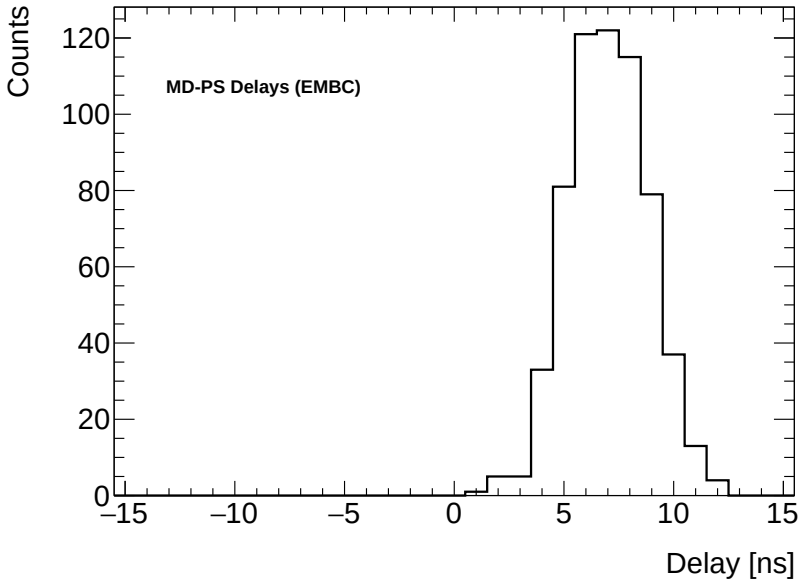


Figure A.1: The distribution shows the MD-PS delay distribution for trigger tower in the EMBC already equipped with LTDBs.

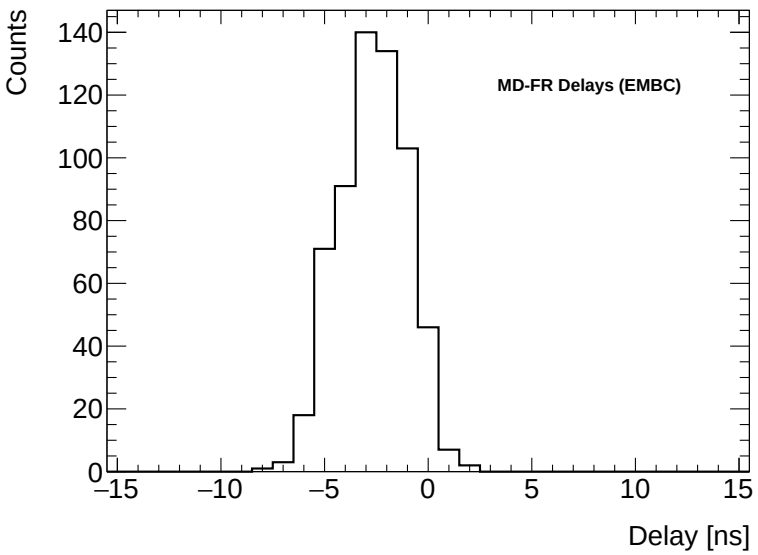


Figure A.2: The distribution shows the MD-FR delay distribution for trigger tower in the EMBC already equipped with LTDBs.

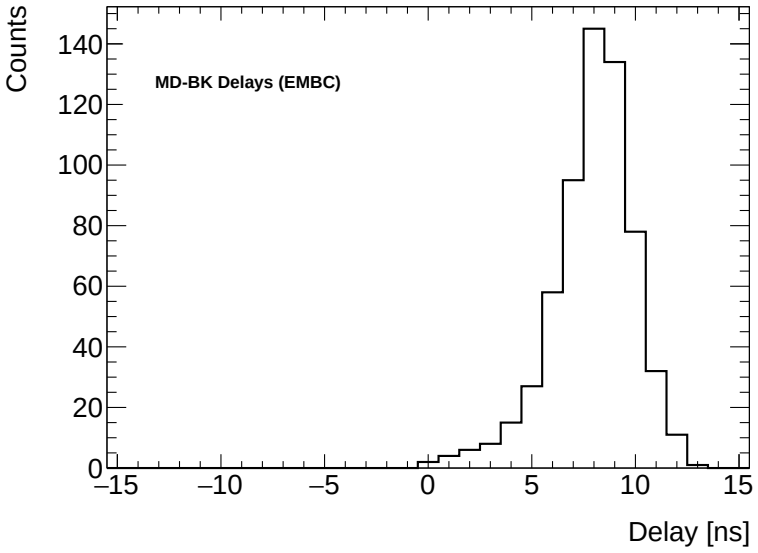


Figure A.3: The effect of the LTDBs onto the delay between the middle and back layer is shown for the EMBC.

# Appendix B

# Abbreviations

CERN - Conseil européen pour la recherche nucléaire
LHC - Large Hadron Collider
LS - Long Shutdown
YETS - Year-End Technical Stop
L1Calo - Level 1 Calorimeter
CTP - Central Trigger Processor
TTC - Timing Trigger and Control
LAr - Liquid Argon
TT - Trigger Tower
PS - Presampler
FR - Front Layer
MD - Middle Layer
BK - Back Layer
SCA - Switch-Capacitor Array
ADC - Analogue to Digital Converter
DAC - Digital to Analog Converter
LSB - Layer Sum Board
TBB - Tower Builder Board
LTDB - Liquid Argon Trigger Digitizer Board
LDPS - Liquid Argon Digital Processing System
ROD - Readout Driver
PPM - Preprocessor Module
(n)MCM - (new) Multi-Chip Module
EMB - Electromagnetic Barrel
EMEC - Electromagnetic Endcap
FCAL - Forward Calorimeter
Tile - Hadronic Detector System in 0 <
HEC - Hadronic Endcap

# Acknowledgements

First and foremost, I want to thank Prof. Dr. Hans-Christian Schultz-Coulon for giving me this opportunity to work in such a large international project with this amazing group of people and his ongoing support.
I also want to thank Dr. Martin Wessels who helped me get to know the L1Calo system and greatly explained everything I needed to know around the ATLAS experiment.
Additionally, I would like to give thanks to Philipp for helping me with everyday questions and proofreading this thesis as well as our constructive discussions.
On top of that, I would like to thank Falk, Martin, Fernando, Tigran and Lisa for their input.
Furthermore, I would like to thank everyone in the ATLAS group at KIP for helping me with all the questions I had.
I also want to thank my friend Julia for always supporting me.
Finally, I am also grateful for my parents' help, who support me and my work as well.

# Bibliography


[1] LHC Design Report Vol.1: The LHC Main Ring. 6 2004. doi: 10.5170/CERN-2004-003-V-1.

[2] The ATLAS Collaboration et al. The ATLAS experiment at the CERN large hadron collider. *Journal of Instrumentation*, 3(08):S08003–S08003, aug 2008. doi: 10.1088/1748-0221/3/08/s08003. URL `https://doi.org/10.1088/1748-0221/3/08/s08003`.

[3] *ATLAS liquid-argon calorimeter: Technical Design Report*. Technical Design Report ATLAS. CERN, Geneva, 1996. URL `https://cds.cern.ch/record/331061`.

[4] G. Aad, T. Abajyan, B. Abbott, J. Abdallah, S. Abdel Khalek, A.A. Abdelalim, O. Abdinov, R. Aben, B. Abi, M. Abolins, and et al. Observation of a new particle in the search for the standard model higgs boson with the atlas detector at the lhc. *Physics Letters B*, Sep 2012. ISSN 0370-2693. doi: 10.1016/j.physletb.2012.08.020. URL `http://dx.doi.org/10.1016/j.physletb.2012.08.020`.

[5] Rende Steerenberg. Lhc report: Another run is over and ls2 has just begun, 2018. URL `https://home.cern/news/news/accelerators/lhc-report-another-run-over-and-ls2-has-just-begun`.

[6] ATLAS Collaboration. Technical Design Report for the Phase-I Upgrade of the ATLAS TDAQ System. Technical Report CERN-LHCC-2013-018. ATLAS-TDR-023, Sep 2013. URL `https://cds.cern.ch/record/1602235`. Final version presented to December 2013 LHCC.

[7] M (CERN) Aleksa, W (Pittsburgh) Cleland, Y (Tokyo) Enari, M (Victoria) Fincke-Keeler, L (CERN) Hervas, F (BNL) Lanni, S (Oregon)

Majewski, C (Victoria) Marino, and I (LAPP) Wingerter-Seez. ATLAS Liquid Argon Calorimeter Phase-I Upgrade Technical Design Report. Technical Report CERN-LHCC-2013-017. ATLAS-TDR-022, Sep 2013. URL `http://cds.cern.ch/record/1602230`. Final version presented to December 2013 LHCC.

[8] G. Aad, B. Abbott, D.C. Abbott, A. Abed Abud, K. Abeling, D.K. Abhayasinghe, S.H. Abidi, O.S. AbouZeid, N.L. Abraham, H. Abramowicz, and et al. Performance of the upgraded preprocessor of the atlas level-1 calorimeter trigger. *Journal of Instrumentation*, 15(11):P11016–P11016, Nov 2020. ISSN 1748-0221. doi: 10.1088/1748-0221/15/11/p11016. URL `http://dx.doi.org/10.1088/1748-0221/15/11/P11016`.

[9] R Achenbach, P Adragna, V Andrei, P Apostologlou, B Åsman, C Ay, B M Barnett, B Bauss, M Bendel, C Bohm, J R A Booth, I P Brawn, P Bright Thomas, D G Charlton, N J Collins, C J Curtis, A Dahlhoff, A O Davis, S Eckweiler, J P Edwards, E Eisenhandler, P J W Faulkner, J Fleckner, F Foehlisch, J Garvey, C N P Gee, A R Gillman, P Hanke, R P Hatley, S Hellman, A Hidvégi, S J Hillier, K Jakobs, M Johansen, E E Kluge, M Landon, V Lendermann, J N Lilley, K Mahboubi, G Mahout, A Mass, K Meier, T Moa, E Moyse, F Mueller, A Neusiedl, C Noeding, B Oltmann, J M Pentney, V J O Perera, U Pfeiffer, D P F Prieur, W Qian, D L Rees, S Rieke, F Ruehr, D P C Sankey, U Schaefer, K Schmitt, H C Schultz-Coulon, C Schumacher, S Silverstein, R J Staley, R Stamen, M C Stockton, S Tapprogge, J P Thomas, T Trefzger, P M Watkins, A Watson, P Weber, and E E Woehrling. The ATLAS level-1 calorimeter trigger. *Journal of Instrumentation*, 3(03): P03001–P03001, mar 2008. doi: 10.1088/1748-0221/3/03/p03001. URL `https://doi.org/10.1088/1748-0221/3/03/p03001`.

[10] Valerie Lang. Praezisionssynchronisierung des level-1-kalorimetertriggers am atlas-experiment. Diplomarbeit, Universität Heidelberg, 2010.

[11] Claire Antel. *Enhancing low mass dark matter mediator resonance searches with improved triggering in the ATLAS detector*. PhD thesis, Universität Heidelberg, 2019.

# Erklärung

Ich versichere, dass ich diese Arbeit selbstständig verfasst habe und keine anderen als die angegebenen Quellen und Hilfsmittel benutzt habe.

Heidelberg, den (Datum) 01.04.2021 .....